Biophysical Journal
Article

Biophysical Society

EPA and DHA differentially modulate membrane elasticity in the presence of cholesterol

Miranda L. Jacobs,[1,2] Hammad A. Faizi,[3] Justin A. Peruzzi,[4,5] Petia M. Vlahovska,[6] and Neha P. Kamat[1,4,*]
[1]Department of Biomedical Engineering, [2]Interdisciplinary Biological Sciences Program, [3]Department of Mechanical Engineering, [4]Center for Synthetic Biology, [5]Department of Chemical and Biological Engineering, and [6]Department of Engineering Sciences and Applied Mathematics, McCormick School of Engineering and Applied Science, Northwestern University, Evanston, Illinois

ABSTRACT Polyunsaturated fatty acids (PUFAs) modify the activity of a wide range of membrane proteins and are increasingly hypothesized to modulate protein activity by indirectly altering membrane physical properties. Among the various physical properties affected by PUFAs, the membrane area expansion modulus (K_a), which measures membrane strain in response to applied force, is expected to be a significant controller of channel activity. Yet, the impact of PUFAs on membrane K_a has not been measured previously. Through a series of micropipette aspiration studies, we measured the apparent K_a (K_{app}) of phospholipid model membranes containing nonesterified fatty acids. First, we measured membrane K_{app} as a function of the location of the unsaturated bonds and degree of unsaturation in the incorporated fatty acids and found that K_{app} generally decreases in the presence of fatty acids with three or more unsaturated bonds. Next, we assessed how select ω-3 PUFAs, eicosapentaenoic acid (EPA) and docosahexaenoic acid (DHA), affect the K_{app} of membranes containing cholesterol. In vesicles prepared with high amounts of cholesterol, which should increase the propensity of the membrane to phase segregate, we found that inclusion of DHA decreases the K_{app} in comparison to EPA. We also measured how these ω-3 PUFAs affect membrane fluidity and bending rigidity to determine how membrane K_{app} changes in relation to these other physical properties. Our study shows that PUFAs generally decrease the K_{app} of membranes and that EPA and DHA have differential effects on K_{app} when membranes contain higher levels of cholesterol. Our results suggest membrane phase behavior and the distribution of membrane-elasticizing amphiphiles impact the ability of a membrane to stretch.

SIGNIFICANCE Polyunsaturated fatty acids (PUFAs) have been shown to have both cardioprotective and neuroprotective effects. Although the mechanism is not well understood, the ability of PUFAs to rapidly integrate into biological membranes and change their mechanical properties may play an important role in biological functions. In this work, micropipette aspiration of vesicle membranes was used to study the effect of several PUFAs on physical properties of DOPC model membranes. Specifically, we showed that EPA and DHA have different effects on membrane elasticity in membranes prepared in the presence of high amounts of cholesterol or nanodomain-forming membranes. This knowledge helps to explain the effects PUFAs may have on cellular membrane elasticity and provides new insight into the role of lipid phase segregation in modulating force transmission.

INTRODUCTION

Polyunsaturated fatty acids (PUFAs) are known to affect many biological processes in diverse cell types, from T cells and endothelial cells to deep-sea bacteria (1,2). Mounting evidence supports the beneficial effects of certain ω-3 PUFAs, in particular, on cardiovascular and neurological systems (3,4). Interestingly, PUFAs have been shown to alter cellular and tissue function by altering the activity of a diverse set of membrane proteins ranging from G-protein coupled receptors (GPCRs) and sodium-potassium pumps to mechanosensitive channels (5,6). The mode of action of PUFAs is still unclear and may be driven through direct interactions of the fatty acids with a site on the membrane protein of interest or through indirect effects achieved through physical changes to membrane structure and properties (6–8).

PUFAs have the ability to change membrane composition and, in effect, membrane properties. Studies of both synthetic and model membranes have shown that PUFAs can rapidly insert into membranes at very fast timescales to alter membrane composition (9) and affect a variety of

Submitted December 5, 2020, and accepted for publication April 9, 2021.
*Correspondence: nkamat@northwestern.edu
Editor: Rumiana Dimova.
https://doi.org/10.1016/j.bpj.2021.04.009

membrane properties (10–12). In particular, the ω-3 PUFAs, eicosapentaenoic acid (EPA) and docosahexaenoic acid (DHA), are two fatty acids that have been shown to affect the stability of phase-segregated domains (13–17), membrane fluidity (18), bending rigidity (19), and hydrophobic thickness (13,18,20) of membranes. Accordingly, PUFAs may impact a variety of biological functions through the modulation of these membrane properties.

Despite the chemical similarities of EPA and DHA, they have been shown to dissimilarly alter the activity of certain membrane proteins. In particular, PUFAs have been shown to differentially affect mechanosensitive channel protein activity (19). Many of these proteins follow the force-from-lipids principle, which suggests that alterations in membrane forces influence the energy needed to drive conformational rearrangements required for protein activity, thus affecting protein function (21). Accordingly, changes in membrane properties that affect how a membrane deforms or transmits forces are likely to affect the activity of embedded mechanosensitive proteins (22). Proteins like Piezo1, TRPV4, and MscL, in addition to others, have been shown be affected by ω-3 PUFAs, becoming activated or inhibited depending on fatty acid identity (5,19,23). Previous studies on membrane physical characterization focused on the impact of EPA and DHA on bending rigidity, fluidity, and hydrophobic thickness (13,18–20,24,25) and had yet to uncover major differences in membrane properties that could be driving these PUFA-induced alterations in protein activity.

One membrane property that is important for membrane protein function is the ability of the membrane to stretch in response to tension. The area expansion modulus (K_a) describes the energy associated with a change in effective spacing between molecules in a lipid bilayer (26). Membrane K_a is likely an important property for mechanosensitive channel activity because it determines the extent of membrane deformation in the same plane upon which channel opening occurs (27,28). However, the direct impact of PUFAs on K_a and the resulting impact on a wide class of mechanosensitive channels has not yet been characterized. To narrow this knowledge gap, it is important to first elucidate how various PUFAs affect membrane area expansion.

In our study, we measure the apparent area expansion modulus (K_{app}) of model membranes containing PUFAs like EPA and DHA. Membrane K_{app} is similar to K_a but does not account for the contribution of residual thermal undulations as the bilayer stretches and is a more accurate term to use when reporting uncorrected micropipette aspiration area expansion data taken in the high-tension regime (29,30). Using micropipette aspiration of model membranes composed of phospholipids, cholesterol, and nonesterified fatty acids, we demonstrate the impact of several PUFAs on membrane K_{app}. In particular, we take a closer look at how PUFAs affect membrane K_{app} in the presence and absence of cholesterol, which affects the propensity of membranes to phase segregate. Our study suggests that membrane phase-segregation behavior and the resulting distribution of membrane amphiphiles may impact the global mechanical properties of membranes, such as K_{app}. We propose that, in turn, these changes in membrane properties may be felt by a wide range of force-sensitive membrane proteins.

MATERIALS AND METHODS

1,2-dioleoyl-*sn*-glycero-3-phosphocholine (DOPC), cholesterol, and 18:1 1,2-dioleoyl-*sn*-glycero-3-phosphoethanoamine-N-(lissamine rhodamine B sufonyl) ammonium salt were purchased from Avanti Polar Lipids, (Alabaster, AL). NBD-phosphoethanolamine, triethylammonium salt was obtained from Thermo Fisher Scientific (Waltham, MA). Oleic acid (OA), α-linoleic acid (ALA), γ-linoleic acid (GLA), stearidonic acid (SDA), DHA, EPA, phosphate-buffered saline (PBS), β-casein, and D-sucrose were purchased from Millipore Sigma (St. Louis, MO). Fatty acid integrity was preserved to the best of our abilities via nitrogen treatment of buffers, storing fatty acids on ice, and limiting aspiration times at room temperature to 1 h immediately after vesicle preparation. Aspiration measurements were conducted on the same day as vesicle preparation.

Thin film hydration

Small unilamellar vesicles (SUVs) were prepared using thin film hydration techniques as described previously (31). Phospholipid-fatty-acid-blended vesicles were prepared by mixing amphiphiles in a chloroform stock solution (32). Briefly, lipid stocks in chloroform were prepared with the indicated mol% of lipids and fatty acids. Samples were dried under nitrogen, then vacuum, for 4 h. To help maintain the integrity of the fatty acids, samples were rehydrated to 10 mM final total lipid in 300 mOsm PBS at 4°C overnight, then brought to 60°C for 5 min. Vesicles were vortexed and extruded seven passes to 100 nm and used immediately.

Electroformation

Giant unilamellar vesicles were prepared using electroformation techniques. A Vesicle Prep-Pro (Nanion Technologies, Munich, Germany) was used to generate giant unilamellar vesicles (GUVs) as described previously. Briefly, 0.05 μmol lipid dissolved in chloroform was dotted onto an indium tin oxide (ITO) slide (Nanion Technologies). Chloroform was dried under vacuum for 20 min. Films were hydrated with 250 μL of 300 mOsm sucrose to a final concentration of 200 μM total lipid and were electroformed using the standard setting (2:18:00 h/min/s, 3 V, 5 Hz, 45°C). After electroformation, samples were diluted in equiosmolar PBS for microscopy studies to both allow vesicles to sink to the surface of the glass slide and ensure fatty acid concentration is below the critical micelle concentration.

Micropipette aspiration

Apparent membrane area expansion modulus (K_{app}) was measured using micropipette aspiration techniques (33,34). Briefly, borosilicate glass capillaries (World Precision Instruments, Sarasota, FL) were pulled to form long, thin tips with minimal change in thickness on the length scale visible during microscopy. Tips were further broken with a microforge to create a blunt end with a diameter of 5–8 μm. Pipettes and sample chambers were incubated in a blocking solution of 5 mg/mL β-casein for 1 h. The pipette was filled with 300 mOsm PBS (pH 7.4). An imaging chamber was assembled using two pieces of 50 × 25 no 1.5 coverglass spaced with vacuum grease. Blocked surfaces were rinsed with 1 mL of 300 mOsm PBS (pH 7.4) three times, and 1 mL was used to fill the imaging chamber. 200 μM

total lipid was used to form GUVs. 1 μL of GUV solution was added to the chamber to an estimated final concentration of 0.2 μM lipid.

The total fatty acid concentration of vesicles in sample conditions used for micropipette aspiration was estimated to be no more than 0.05 μM fatty acid, which is below the critical micelle concentration of OA. Below the critical micelle concentration, fatty acid is expected to favor partitioning into the bilayer (9,35,36). Notably, it appears that there is a significant reduction in the amount of fatty acid that actually resides in the membrane ($\sim$5 mol%) relative to the amount included in the original chloroform stock solution used to prepare lipid films (25 mol%), indicating fatty acid is lost to the surrounding solution during vesicle formation. Micropipette aspiration measurements were performed on two to five independent GUV samples, and the total number of aspirated vesicles per composition is included in tabular results. Sucrose is known to affect membrane properties (37) but improves membrane contrast and decreases vesicle mobility in the imaging chamber. For these reasons, sucrose was required for micropipette aspiration to easily capture the vesicles and visualize the membrane within the glass micropipette. It is important to note that changing the salt and sugar conditions of micropipette aspiration conditions will alter the measured mechanical properties of bilayers. Our measurements of bending rigidity via fluctuation spectroscopy used sucrose-free conditions. These measurements match the bending rigidity values extracted from micropipette aspiration conducted with sucrose-containing vesicles, indicating the particular solvents used had little effect on the bending rigidity of vesicles relative to one another.

Using a Nikon inverted microscope (Nikon, Melville, NY), connected to a Validyne pressure transducer and digital manometer (model DP 15-32; Validyne Engineering, Northridge, CA) and a micromanipulator (model WR-6; Narishige International USA, Amityville, NY), vesicles free of visible defects between 10 and 60 μm were gently aspirated with a micropipette prepared as described above. Membranes were carefully prestressed (29) for 30 s to approximately half-maximal tension (around 2–4% areal strain) before bursting to remove any invisible membrane folds. Samples with visible membrane folds or other defects were not used because they tend to exhibit different responses to membrane stretching because of membrane reservoirs, resulting in artificially low K_a-values. After prestress, suction pressure was reduced to baseline. If large amounts of hysteresis occurred, vesicles were prestressed again or discarded because this indicates large amounts of excess membrane. Vesicles were then aspirated at 2 cm H_2O increments and imaged every 10 s. Images were analyzed using Fiji (38) to measure pipette diameter, vesicle area, and change in vesicle area within the pipette. Membrane K_{app} was calculated for each composition from the slope of the percent area dilation within the pipette ($\Delta A/A_o$) and membrane tension (τ).

$$K_{app} = \frac{\tau}{\frac{\Delta A}{A_o}}, \tag{1}$$

where ΔA is the change in area of membrane within the micropipette and A_o is the initial area of the aspirated vesicle within the pipette. The average K_{app} from at least 10 vesicles was used to calculate mean K_{app}-values, and the actual N is reported with each mean K_{app}. Ordinary one-way ANOVA multiple comparisons tests were used to determine significance between compositions.

Fluctuation spectroscopy

GUVs formed using electroformation were analyzed using the flickering spectroscopy method (39) to measure membrane bending rigidity. The harvested vesicles were diluted 10 times in a slightly higher concentration of 270 mM sucrose + 60 mM glucose solution to obtain deflated vesicles. This combination of sucrose and glucose provides a good optical contrast for contour detection (40) and avoids gravitational effects on vesicle fluctuations (41). The equatorial membrane fluctuations were recorded with phase contrast microscope (Axio-Observer A1 microscope; Carl Zeiss AG, Oberkochen, Germany) using a 63×/NA 0.75 Ph2 (air) objective. The focal depth, FD, was determined using the standard formula,

$$d = \frac{\lambda}{NA^2}, \tag{2}$$

where the wavelength, λ, of transmission light is 550 nm. This leads to $FD = 0.97$ μm and the nondimensionalized $\Delta = FD/R_o$ (vesicle size range of radius, R_0, 20–50 97 μm) smaller than 0.05 to avoid the averaging effect of out of focus optical projections on equatorial projections (42,43). 8000–10,000 images were recorded at 60 frames per second with a Photron SA1.1 high-speed camera (Photron USA, San Diego, CA) with a shutter speed of 200 μs. The imaging acquisition speed was later adjusted to avoid time correlation between Fourier modes (44) for every specific vesicle. The contour in the equatorial plane of a quasispherical vesicle is decomposed in Fourier modes,

$$r(\phi, t) = R_0\left(1 + \sum_{q=-q_{max}}^{q_{max}} u_q(t)\exp(iq\phi)\right), \tag{3}$$

where q is the resolved Fourier mode. In general, q_{max} is the maximal number of experimentally resolved modes that is dependent on the optical resolution of the camera. The mean-square amplitude of the fluctuating amplitudes, u_q, yields the values of membrane bending rigidity κ and the tension σ because

$$\left\langle \left| u_q \right|^2 \right\rangle \sim kT/\kappa\left(q^3 + \overline{\sigma}q\right), \tag{4}$$

where $\overline{\sigma} = \sigma R_0^2$. To have good sensitivity with bending rigidity measurements, only vesicles with low tension value were chosen, ranging from 10^{-8} to 10^{-9} N/m. This ensures a small crossover mode defined by

$$q_c = \sqrt{\overline{\sigma}} \tag{5}$$

from $q = 3$ to 7. Shape fluctuation modes $q < q_c$ are dominated by membrane tension, whereas modes $q > q_c$ are controlled by bending rigidity.

RESULTS

ω-3 fatty acids increase membrane elasticity in the absence of cholesterol

We first set out to understand how nonesterified or free fatty acids (FFAs) impact the membrane area expansion modulus of model DOPC phospholipid membranes as a function of fatty acid content, identity, and the presence of varying amounts of cholesterol. We measured the apparent expansion modulus (K_{app}), which is the slope of tension versus apparent area dilation measured during micropipette pressurization of vesicles in the high-tension regime (Fig. 1 *A*). Membrane K_{app} is similar to K_a but does not account for the contribution of residual thermal undulations as the bilayer stretches and is a more accurate term to use when reporting uncorrected micropipette aspiration area expansion data taken in the high-tension regime (29,30). Using electroformation techniques, we prepared multicomponent GUVs from chloroform stock solutions containing phospholipids, cholesterol, and nonesterified fatty acids. We were able to include up to 25

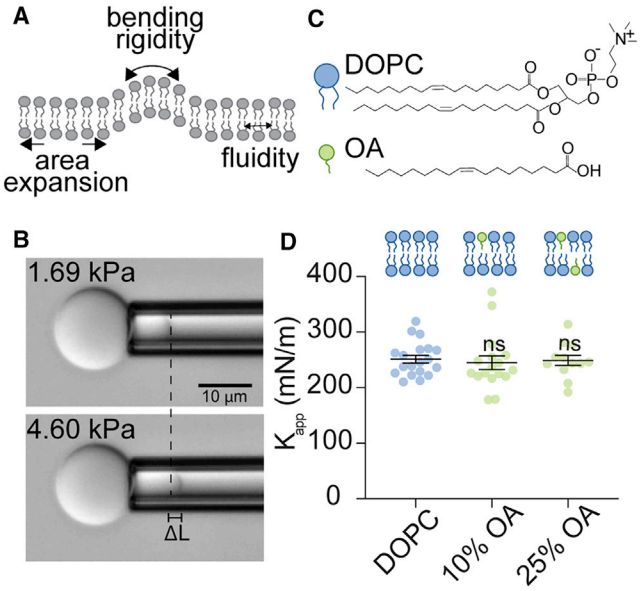

FIGURE 1 Apparent area expansion moduli (K_{app}) of model membranes containing nonesterified fatty acids. (*A*) In the course of this study, we measured three membrane mechanical properties including apparent area expansion modulus (K_{app}), bending rigidity (k_c), and fluidity. (*B*) Example images of a micropipette aspiration study used to measure K_{app}. GUVs are aspirated into glass micropipettes where applied pressure induces membrane tension. Membrane stretching can be quantified by a change in vesicle projection length within the pipette (ΔL). Scale bar, 10 μm. (*C*) Chemical structures and schematics of DOPC and OA. (*D*) Incorporation of OA does not alter the K_{app} of DOPC membranes. Increasing OA content in lipid stocks, from DOPC (no FA) to 25% OA in DOPC membranes, does not impact K_{app}. Dots represent K_{app}-values from a single vesicle aspiration. Black lines represent mean K_{app}, error bars represent standard error of the mean, and $n \geq 12$ vesicles were aspirated per composition. Vesicle assembly was disrupted above 25% OA incorporation. Micropipette aspiration studies were conducted in PBS (pH 7.4). *p*-values were generated by ANOVA using Dunnett's multiple comparisons test compared to DOPC, nonsignificant (ns) $p > 0.5$.

mol% FFAs in the lipid solutions used to prepare vesicles; higher amounts of FFA in the lipid stock solution inhibited the formation of vesicles. We chose to incorporate FFAs into vesicles by premixing them with phospholipids in a chloroform solution before vesicle assembly (45) instead of adding them to preformed vesicles, as has typically been done (18). We used this alternate incorporation method to avoid the introduction of cosolvents such as ethanol that are typically required to solubilize fatty acids but are also expected to change membrane properties. Using an absorbance-based lipid oxidation assay and mass spectrometry, we determined that under our experimental conditions, fatty acid oxidation is expected to be limited over the timescale of vesicle formation and aspiration (Fig. S1; Table S1; (29,46)). We then used differential interference contrast microscopy to visualize GUVs in the tip of a micropipette and measured the changes in vesicle area within the pipette as pressure was applied (Fig. 1 *B*). This aspiration procedure provided us with a stress-strain response curve, the slope of which was used to determine the K_{app} (Eq. 1) of various membrane compositions (Fig. S2).

Next, we measured FFA incorporation into the DOPC membranes after vesicle formation. Fatty acid incorporation efficiency was dependent on fatty acid identity. Lipid stock solutions were made in chloroform to contain 75 mol% DOPC and 25 mol% of various fatty acids with differing hydrocarbon chain length and unsaturation. Using FFA and phospholipid quantification kits (Supporting materials and methods), we found that a monounsaturated fatty acid, OA, included in the chloroform stock solution at 25 mol% was subsequently incorporated into the bilayer at 15 mol%. Polyunsaturated FFAs such as EPA and DHA were incorporated around 5 mol% (Fig. S3). In addition, we performed lipidomic analysis on our vesicles to further quantify our membrane compositions (Table S1). We found, using the more sensitive method of mass spectrometry, that each FFA incorporated around 7 mol% relative to DOPC. Because the polyunsaturated fatty acids, EPA and DHA, were incorporated into vesicle membranes at similar levels, we proceeded to compare changes in membrane properties between vesicles containing different polyunsaturated FFAs.

Because fatty acids have differing hydrophilic headgroups and a smaller cross-sectional area compared to diacyl phospholipids, we first measured the impact of FFA headgroup on vesicle membrane K_{app}. FFAs consist of a carboxylic acid headgroup with a single hydrocarbon chain, and phospholipid molecules consist of a phosphocholine headgroup and two hydrocarbon chains (Fig. 1 *C*). To isolate the effects of the carboxyl headgroup on K_{app}, we prepared DOPC (18:1) vesicles with increasing fractions of OA (18:1) such that we retained the identity of hydrocarbon chains in the membrane (13). We observed that OA content did not impact membrane K_{app} when up to 25 mol% OA was included in the lipid stock solution (Fig. 1 *D*). These results indicate that the carboxylic acid headgroup and single-chain structure of FFAs do not alter the K_{app} of membranes with the same hydrocarbon chain composition.

We then wondered how the identity of the hydrocarbon chain of FFAs, including length, unsaturation content, and position of unsaturation, would impact membrane K_{app}. First, we compared GLA (18:3) and ALA (18:3), an ω-6 and ω-3 fatty acid, respectively (Fig. 2 *A*). These fatty acids were selected because of their three unsaturated bonds and identical chain length but differing location of their unsaturated bonds along their hydrocarbon chain, which allowed us to determine the effect of the location of unsaturated bonds in a fatty acid on membrane K_{app}. When OA, GLA, and ALA were included in DOPC lipid stock solutions at 25 mol%, we found that GLA and ALA reduced K_{app} (200 and 197 mN/m, respectively) to a similar extent compared to both OA-containing (249 mN/m) and pure DOPC membranes (245 mN/m) (Fig. 2 *B*; Table 1). These results indicate that for fatty acids containing three unsaturated bonds, the location of unsaturation at either the ω-6 or

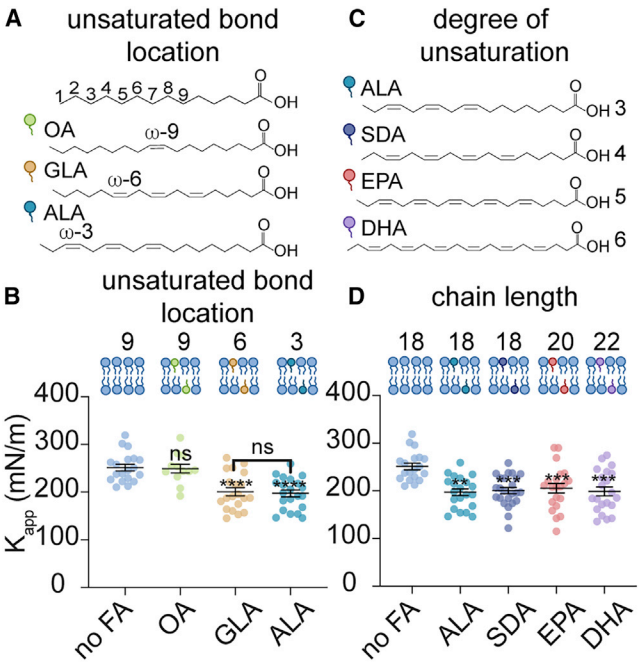

FIGURE 2 Effect of the number and position of unsaturated bonds in nonesterified PUFAs on K_{app}. (*A*) Chemical structures and schematics of OA, GLA, and ALA. Selected fatty acids are ω-9, 6, and 3, respectively. (*B*) Membrane K_{app} is reduced equally in the presence of GLA and ALA compared to no FA and OA. (*C*) Chemical structures and schematics of polyunsaturated ω-3 fatty acids ALA, SDA, EPA, and DHA. (*D*) K_{app} is reduced similarly in membranes containing ω-3 polyunsaturated fatty acids with three or more unsaturated bonds, regardless of the hydrocarbon chain length and number of unsaturated bonds. (*B* and *D*) Micropipette aspiration measurements were conducted on vesicles prepared using lipid stocks containing 100% DOPC (no FA) or 75 mol% DOPC, 25 mol% FA. Error bars represent standard error of the mean. *p*-values were generated by ANOVA using Dunnett's multiple comparisons test compared to no FA. n $\geq$ 12 vesicles were aspirated per composition, ****$p \leq 0.0001$, ***$p \leq 0.001$, **$p \leq 0.01$, ns $p > 0.5$.

ω-3 position does not impact the K_{app} of DOPC membranes. Next, we investigated how the chain length and degree of unsaturation of FFAs impact membrane K_{app}. Using ω-3 fatty acids ALA (18:3), SDA (20:4), EPA (20:5), and DHA (22:6), we analyzed how simultaneously increasing the degree of unsaturation as well as the chain length of a fatty acid affected membrane K_{app} (Fig. 2 *C*). We found that each polyunsaturated fatty acid decreased membrane K_{app} to a similar extent ($\sim$200 mN/m) compared to pure DOPC membranes (245 mN/m) (Fig. 2 *D*; Table 1). Thus, increasing the extent of unsaturation and chain length in ω-3 fatty acids containing at least three unsaturated bonds appears to have no further effect on membrane area expansion moduli in DOPC model membranes. To the best of our knowledge, these results are the first K_{app} measurements of vesicles containing FFAs and are consistent with previous findings performed with phospholipid-conjugated fatty acids (29,47).

We next set out to validate the effect of FFAs on membrane fluidity, a property that has been studied more extensively in the presence of fatty acids. Using diphenylhexatriene (DPH) fluorescence anisotropy of SUVs, we measured the relationship between membrane fluidity and FFA identity in DOPC model membranes. We found that that FFAs generally increase membrane fluidity (Fig. S4). This result is consistent with previous studies that measured the effect of unsaturated fatty acid integration, both when the FA was a phospholipid conjugate and as an FFA, on the fluidity of model and cellular membranes (19,45,48). However, in this study, we expanded the range of FFA molecules explored. Furthermore, we observed that as the number of unsaturated bonds increases, fluidity is increased to a greater extent (Fig. S4). Taken together, our results indicate that FFAs generally increase the fluidity and decrease the K_{app} of DOPC model membranes as a function of their unsaturated bond content.

EPA and DHA differentially affect membrane elasticity in the presence of high levels of cholesterol

We next wondered how FFA inclusion would affect the K_{app} of membranes containing cholesterol. Cholesterol is a sterol found in all eukaryotic cell types and is critical for the proper function of a diverse array of membrane proteins. Among its many effects, this molecule promotes the formation of phase-segregated nanometer-sized crystalline domains, known as lipid rafts (49,50), which have been found to affect the location and activity of membrane proteins (12,20,22,51,52). At low mole fractions, cholesterol is soluble and is dispersed through a bilayer membrane (18,53). As the mole fraction of cholesterol increases to around 50 mol%, as in the lipid mixtures we investigated, the area fraction and number of cholesterol-rich crystalline domains also increases (18,49,54,55). Using ternary mixtures of fatty acids, cholesterol at either low (25 mol% stock solution) or high (45 mol% stock solution) amounts, and DOPC, we sought to determine how FFAs affected membrane K_{app} when cholesterol was present.

We first prepared vesicles containing a low amount of cholesterol from stock solutions containing 25 mol% fatty acid, 25 mol% cholesterol, and 50 mol% DOPC and performed micropipette aspiration studies (Fig. 3 *A*). At this

TABLE 1 K_{app}-values of fatty acid/DOPC blended membranes

	DOPC	10% OA	25% OA	25% GLA	25% ALA	25% SDA	25% EPA	25% DHA
K_{app} (mN/m)	251 ± 7	245 ± 12	249 ± 9	200 ± 9	197 ± 7	200 ± 7	205 ± 10	199 ± 10
n	19	17	12	20	21	24	21	21

K_{app}-values were measured using micropipette aspiration techniques. Vesicles were constructed from lipid stocks containing DOPC and varying mol percentages of each fatty acid, which are listed in the table. Values are represented as standard error of the mean (SEM). The number of aspirated vesicles is included for each composition.

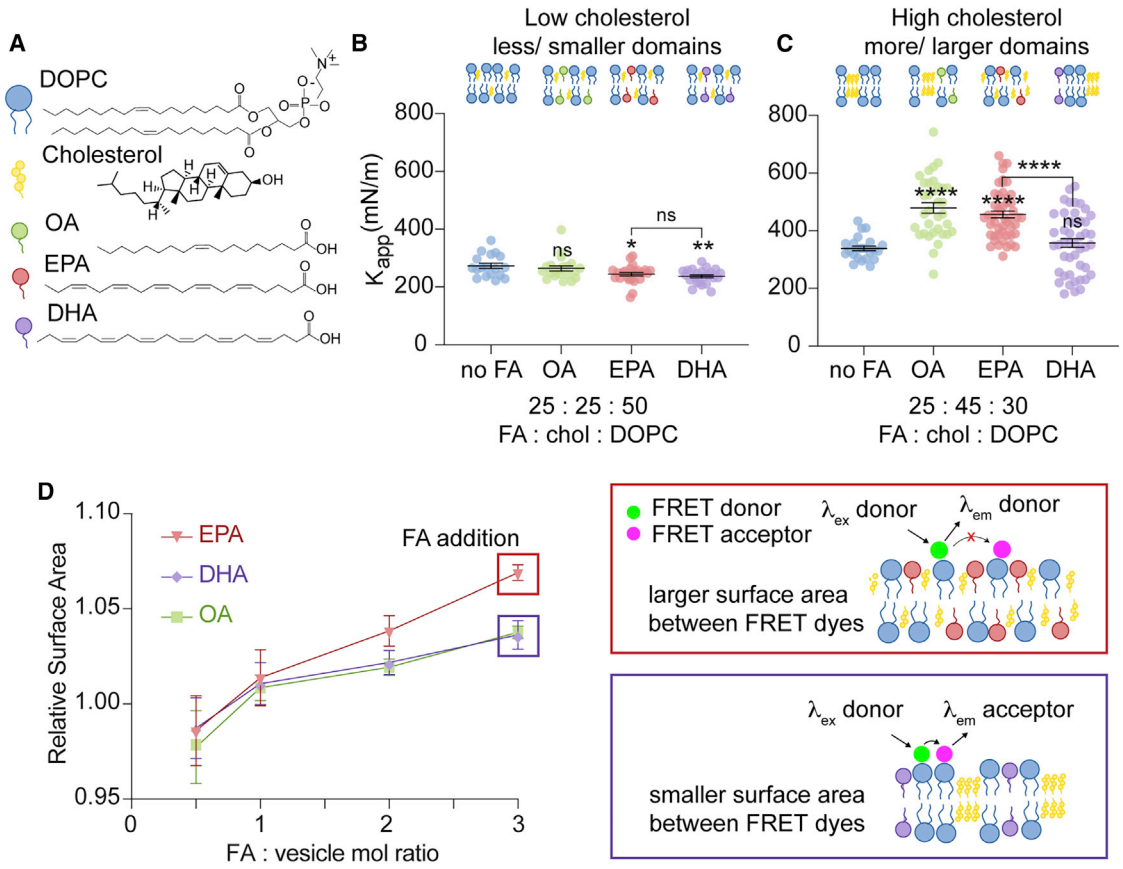

FIGURE 3 DHA and EPA have distinct effects on the K_{app} of membranes with cholesterol nanodomains. (*A*) Chemical structures and schematics of cholesterol, DOPC, and select FAs. (*B*) DOPC membranes have a reduced K_{app} in the presence of EPA and DHA compared to no FA when low amounts of cholesterol are present. Vesicles were constructed from lipid stocks composed of chol/DOPC 25:75 (no FA) and FA/chol/DOPC 25:25:50, n $\geq$ 18. (*C*) DHA decreases the K_{app} of membranes assembled with higher concentrations of cholesterol compared to EPA. Vesicles were constructed from lipid stocks containing chol/DOPC 50:50 (no FA), and FA/chol/DOPC 25:45:30. Error bars represent standard error of the mean, n $\geq$ 23. *p*-values were generated by ANOVA using Dunnett's multiple comparisons test compared to no FA. ****$p \leq 0.0001$, **$p \leq 0.01$, *$p \leq 0.05$, ns $p > 0.5$. (*D*) Bulk FRET measurements of SUVs were used to determine the effect of EPA and DHA on nanodomain disruption. EPA inclusion increases the average distance between FRET-labeled lipids to a greater extent than OA and DHA, suggesting enhanced cholesterol redistribution with EPA. 10 mM 50 mol% chol, 50 mol% DOPC vesicles were prepared with different concentrations of equimolar 18:1 NBD-phosphoethanolamine, triethylammonium salt and 18:1 1,2-dioleoyl-*sn*-glycero-3-phosphoethanoamine-N-(lissamine rhodamine B sufonyl) ammonium salt. The FRET ratio (f_{don}/f_{acc}) demonstrates energy transfer efficiency between the dyes after fatty acid addition. Relative surface area was determined by normalizing the fluorescence intensity of each sample to the fluorescence intensity in fatty-acid-free PBS (data not shown). FRET studies were conducted in 300 mOsm PBS (pH 7.4), n = 3 using independent vesicle samples.

concentration, we expected that cholesterol would not significantly affect lipid segregation and the membrane components would remain well mixed (18,54). We chose to focus our studies on two FFAs, EPA and DHA, because of their biological relevance and distinct effect on membrane protein activity (6,12,19,48,56). As a control, we prepared vesicles with 25 mol% OA because this FFA had not impacted membrane K_{app} when mixed with DOPC in the absence of cholesterol (Fig. 1 *D*). In addition, we chose OA as an elasticity control because a previous study by Bruno and colleagues found that OA did not alter the activity of a mechanosensitive protein, gramicidin (6). Furthermore, OA inclusion also allowed us to control for the smaller physical size of an FFA compared to a phospholipid and the potential physicochemical effects these FFAs may have on membrane properties (13). The inclusion of 25 mol% cholesterol in stock solutions with DOPC slightly increased the K_{app} relative to cholesterol-free membranes as expected (273 mN/m) (33). Our results using OA, EPA, and DHA mimicked those we observed in cholesterol-free membranes. We observed that OA had no effect on the K_{app} of membranes containing low mol% cholesterol (264 mN/m). The subsequent addition of EPA and DHA reduced membrane K_{app} to similar levels (~240 mN/m) with respect to membranes lacking fatty acid (no FA) (273 mN/m) (Fig. 3 *B*; Table 2). These results demonstrated that the inclusion of the FFAs DHA and EPA in membranes containing low mol% cholesterol had a similar effect of reducing membrane K_{app} as they had in membranes without cholesterol (Figs. 1 and 2).

We then investigated how FFA inclusion affected the K_{app} of phospholipid membranes when they contained higher

TABLE 2 K_{app}-values for DOPC membranes containing fatty acids and cholesterol domains

More domains	50 mol%, chol 50%, DOPC	25% OA, 45% chol, 30% DOPC	25% EPA, 45% chol, 30%DOPC	25% DHA, 45% chol, 30% DOPC
K_{app} (mN/m)	339 ± 8	479 ± 18	463 ± 13	357 ± 15
n	23	34	51	46
Fewer domains	25 mol% chol, 75%DOPC	25% OA, 25% chol, 50% DOPC	25% EPA, 25% chol, 50% DOPC	25% DHA, 25% chol, 50% DOPC
K_{app} (mN/m)	273 ± 9	264 ± 9	244 ± 6	237 ± 5
n	18	21	25	23

Sample names indicate the composition of lipid chloroform stocks used to create vesicles. Values are represented as mean ± SE.

levels of cholesterol, which should form a greater amount of cholesterol-rich, crystalline nanodomains. Previous work by Mason et al. using x-ray diffraction analysis demonstrated that EPA and DHA can have distinct effects on cholesterol nanodomains; whereas EPA enhances cholesterol mixing and disrupts domains by integrating into both liquid-ordered and liquid-disordered domains, DHA increases the size and stability of membrane domains because of its exclusion from ordered domains (11,13,18,53,56–59). Yet, we were unsure of how these structural changes would affect the bulk membrane property, K_{app}. We measured the K_{app} of DOPC membranes containing high amounts of cholesterol and OA, DHA, or EPA. In the presence of fatty acids, we were able to include, at most, 45 mol% cholesterol in our lipid stocks because higher amounts of cholesterol prevented vesicle formation. Using GUVs constructed from lipid stocks containing ternary mixtures of 25 mol% fatty acid, 45 mol% cholesterol, and 30 mol% DOPC, we determined that K_{app} increased in the presence of OA (479 mN/m) and EPA (463 mN/m) compared to DOPC/cholesterol alone (339 mN/m) (Fig. 3 *C*; Table 2). We attribute this increase in K_{app} in the presence of OA to an increase in the cholesterol area fraction of the membrane because OA is a single-hydrocarbon-chain lipid, but DOPC contains two chains. When DOPC is replaced with OA, there is more cholesterol per hydrocarbon chain, which is expected to increase K_{app} as if more cholesterol is present (33,60). We expected EPA to reduce membrane K_{app} to a similar extent as DHA, resembling our observations with cholesterol-free and low-cholesterol content membranes. Surprisingly, we observed that EPA increased membrane K_{app} (463 mN/m) compared to DHA (357 mN/m) (Fig. 3 *C*; Table 2). These results indicate that in the presence of high mol% cholesterol, DHA and EPA affect the K_{app} of DOPC membranes differently, which has not been observed previously.

We wondered whether the higher content of cholesterol was affecting the phase-segregation behavior of DOPC model membranes and contributing to the differential effects of DHA versus OA and EPA on membrane K_{app}. We first confirmed that cholesterol inclusion at 50 mol% in preformed membranes exhibited measurable increases in membrane phase segregation with DHA addition compared to EPA addition (Figs. 3 *D* and S5). We assessed changes in phase behavior by monitoring changes in membrane surface area. Using a bulk Förster resonance energy transfer (FRET) assay, we measured the average distance between fluorophore-labeled lipids. In the presence of 50 mol% cholesterol, the fluorophores conjugated to unsaturated phospholipids should colocalize with liquid-disordered domains. Using this FRET assay, we observed larger differences in surface area changes with the external addition of EPA compared to OA and DHA. We attribute the greater FRET change in response to EPA to enhanced disruption of cholesterol domains, which increases the effective surface area of the dye-containing fraction of the membrane as cholesterol mixes with the phospholipids. This result indicated that EPA disrupted cholesterol domains to a greater extent than OA and DHA, leading to greater spacing between FRET-labeled dyes as consistent with previous findings (18). In contrast, in membranes containing low mol% cholesterol, where nanodomains were not expected to occupy a significant fraction of the membrane, we observed no differences in membrane surface area change between EPA and DHA-containing membranes (Fig. S6). These results supported our hypothesis that in membranes containing higher amounts of cholesterol, EPA disrupted phase-segregated domains to a greater extent than DHA.

We set out to better understand why DHA reduced K_{app} relative to EPA when cholesterol was present at high levels in DOPC membranes but induced similar changes in K_{app} when cholesterol was at lower levels or absent. First, we wondered whether the discrepancy in K_{app}-values for membranes containing EPA or DHA was due to differential incorporation of either fatty acid. To test this, we used a phospholipid and a fatty acid quantitation assay to measure our true membrane compositions and found that EPA and DHA were present in similar amounts in their respective membranes (Fig. S7). Interestingly, we observed OA was present at higher levels in electroformed vesicles than DHA or EPA. This difference in incorporation was expected because the partition coefficient of OA is 10 times larger than DHA in DOPC membranes; however, previous studies have demonstrated the potent effects of DHA despite this lower incorporation efficiency (6). However, as OA did not reduce membrane $K_{app,}$ we concluded the differential

level of incorporation of this particular fatty acid did not have a significant impact on our observations. We next explored the possibility that the presence of EPA or DHA differentially affected how much cholesterol was included in the membrane during formation and thereby affected the resulting K_{app}. We used fluorescence microscopy to compare cholesterol content in membranes containing different fatty acids by measuring the fluorescence of a boron-dipyrromethene-labeled-cholesterol. We found that fatty acid content did not affect cholesterol partitioning into electroformed GUVs and that cholesterol was present in similar levels in the different vesicle samples we explored (Fig. S8). We confirmed this result using lipidomic analysis of our vesicles and found that cholesterol incorporated around 10 mol% in the presence of each fatty acid (Table S1). Although this incorporated amount is significantly less than what was included in the lipid stock solution (45 mol%), previous results from Stevens et al. (61) demonstrated that sterol solubility in electroformed membranes may be limited. Although they observed up to 65 mol% cholesterol in assembled membranes, their studies included a different phospholipid, DPPC, which may have increased cholesterol solubility (61). In addition, we do not expect that a change in phase behavior due to force application (62) altered our aspiration results, as studies were performed at room temperature and the calculated phase transition temperature for these compositions is well below that (Fig. S9; Table S2). Taken together, these results suggest that differences in K_{app} between membranes containing DHA versus EPA are not due to differences in molar ratios of the amphiphilic components.

We then investigated if these changes in phase behavior impacted other membrane physical properties beyond K_{app}. Using the flickering spectroscopy method, we measured the bending rigidity (k_c) of vesicles formed from lipid stocks containing 25 mol% fatty acid, 45 mol% cholesterol, and 30 mol% DOPC. We found that EPA and DHA similarly increase k_c compared to OA and membranes without any FFAs (Table 3). This increase in bending stiffness in the presence of fatty acids is consistent with previous studies on model membranes, in which FFAs alter the area per lipid of membrane amphiphiles and the resulting curvature strain increases k_c (45). In addition, our observation of no significant difference between the bending stiffness of EPA- versus DHA-containing membranes is consistent with atomic force microscopy measurements of cells enriched in EPA and DHA (19), though these studies observed a decrease in bending stiffness upon EPA and DHA addition. We were also able to extract k_c-values from the low-tension regime of our micropipette aspiration data. We compared k_c measured by the flickering spectroscopy method and micropipette aspiration and observed similar increases in bending rigidity (Fig. S3; Table S3). Our finding of k_c being unaffected by the presence of cholesterol nanodomains suggests that membrane phase behavior does not impact bulk k_c measurements in a similar manner to K_{app}. This uncoupling of K_{app} and k_c was unexpected, as a decrease in K_{app} is typically concurrent with a decrease in k_c (29). We also measured membrane fluidity in membranes with FFAs in the presence of high amounts of cholesterol. We found that in the presence of high levels of cholesterol, DHA increased membrane fluidity to a greater extent than EPA and compared to no fatty acid (Fig. S10), consistent with previous findings (18). However, this result was also consistent with our findings in cholesterol-free membranes (Fig. S4). Therefore, the K_{app} is the only membrane property that we measured that uniquely exhibits differences between EPA and DHA when in the presence of phase-segregated nanodomains. These results suggest that phase-segregated nanodomains have a pronounced effect on membrane K_{app} compared to k_c and fluidity.

Membrane phase-segregation behavior impacts elasticity with an alternate phospholipid composition

Finally, to investigate this proposal that EPA and DHA differentially alter membrane K_{app} through differentially altering cholesterol crystalline domain behavior, we used an alternate membrane composition that also forms cholesterol nanodomains: 1-palmitoyl-2-oleoyl-glycero-3-phosphocholine (POPC) (18:1, 16:0) and cholesterol. POPC is similar to DOPC except one of its 18-carbon monounsaturated chains is replaced with one 16-carbon saturated chain. We expected to observe similar relationships between cholesterol content and K_{app}-values as a function of FFA identity as we observed in DOPC membranes. Additionally, we expected that the difference in K_{app}-values between EPA and DHA-containing membranes would be more pronounced in POPC membranes because cholesterol has a greater stiffening effect on saturated lipids (33,63). Using micropipette aspiration, we measured the K_{app} of GUVs formed from lipid stocks containing ternary mixtures of 25 mol% fatty acid, 45 mol% cholesterol, and 30 mol%

TABLE 3 k_c-values for fatty acid and cholesterol-containing membranes

	50 mol% chol, 50% DOPC	25% OA, 45% chol, 30% DOPC	25% EPA, 45% chol, 30% DOPC	25% DHA, 45% chol, 30% DOPC
k_c (K_BT)	30.4 ± 2.6	20.8 ± 2.1	33.4 ± 4.3	37.6 ± 3.2
k_c (K_BT)	60.5 ± 5.4	76.9 ± 4.7	72.0 ± 6.8	66.0 ± 5.6

k_c-values were determined using the flickering spectroscopy method and are reported as mean ± standard deviation, $n \geq 15$. Sample names indicate the composition of lipid stocks in chloroform.

POPC. In the POPC membranes made with high cholesterol content, we observed that K_{app} increased in the presence of OA (600 mN/m) and EPA (837 mN/m) compared to membranes containing POPC and cholesterol alone (545 mN/m) (Fig. 4 *A*; Table 4). This result matched the general trends observed with DOPC and high-cholesterol-content membranes (Fig. 3 *C*). Similar to DOPC samples, we found that the K_{app} of DHA-containing POPC membranes (462 mN/m) was significantly reduced compared to membranes that contained EPA (837 mN/m). Lipidomic analysis of these samples revealed that in POPC membranes prepared with high concentrations of cholesterol, EPA and DHA incorporated at similar levels of 2.9 and 3.5 mol%, respectively, whereas OA incorporated at 7.7 mol% (Table S1). These results confirmed that in the presence of high amounts of cholesterol, which is believed to form cholesterol-rich domains, EPA and DHA have significantly different effects on membrane K_{app}. Taken together, our results in POPC/cholesterol and DOPC/cholesterol systems demonstrate that the FFAs EPA and DHA can differentially impact membrane area expansion moduli when cholesterol is present at high amounts.

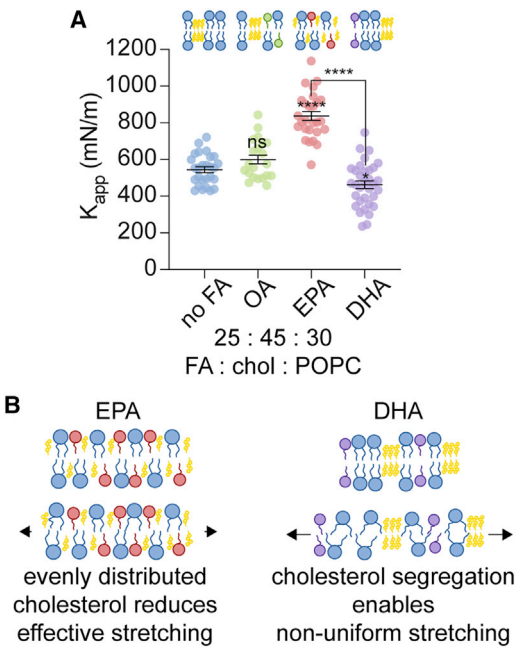

FIGURE 4 Assessing the generality of the effect of cholesterol content on FFA-induced changes in K_{app}. (*A*) POPC vesicles prepared with high (45 mol%) amounts of cholesterol confirm that EPA and DHA have differential effects on membrane K_{app}. K_{app} is reduced in DHA-containing vesicles compared to vesicles containing EPA. Vesicles were constructed from lipid stocks composed of chol/POPC 50:50 (no FA) and FA/chol/POPC 25:45:30 vesicles. Error bars represent standard error of the mean, $n \geq 18$. *p*-values were generated by ANOVA using Dunnett's multiple comparisons test compared to no FA, $^{****}p \leq 0.0001$, $^{*}p \leq 0.05$, ns $p > 0.5$. (*B*) Proposed mechanism of decreased membrane K_{app} in the presence of phase-segregated cholesterol nanodomains.

DISCUSSION

Here, we have shown the effect of FFAs on membrane K_{app} in phospholipid model membranes, which we believe are the first measurements of this nature. As FFAs are increasingly found to alter biological processes, the impact of FFA inclusion on membrane properties is important to understand. FFAs insert at fast timescales, much faster than metabolic-based membrane reorganization (9). Therefore, FFAs have the ability to transiently alter the local membrane composition (64) and impact biological function even before their incorporation in diacyl phospholipids. This would be especially prevalent in cells with malfunctioning machinery to control membrane composition or in cells lacking this machinery, such as red blood cells (65,66). Therefore, understanding the specific role of FFAs on membrane physical properties is important to bridge the gap between FFA effects on membrane composition and their subsequent effects on cellular function.

Our K_{app} results with OA, which has the same hydrocarbon structure as DOPC lipids, indicate that the carboxylic headgroup and single-chain structure of an FFA are not the dominant contributors to FFA-induced changes in K_{app}. Consistent with previous findings that explored the effect of unsaturation in diacyl lipids on the area expansion modulus (29,47), it appears that the extent of hydrocarbon chain unsaturation is a key contributor to shifts in K_{app}. The structure of the fatty acid, whether it is in a monoacyl form or incorporated into a phospholipid, does not appear to matter in this regard. Because introducing double bonds into an amphiphile chain causes thinning of the bilayer (18,29), the membrane should exhibit an increased ability to stretch. This effect of membrane thinning and an increased area per lipid with the inclusion of polyunsaturated fatty acids reduces the energy required for elastic deformation (47). These previous results support our finding that FFA polyunsaturation reduces model membrane K_{app}.

Additionally, we explored how the increasingly investigated ω-3 fatty acids, EPA and DHA, affected membrane K_{app} in the absence and presence of cholesterol. These FFAs, which have similar effects on membrane K_{app} in the presence of no or low cholesterol, have different effects on K_{app} once cholesterol content is increased. For example, when EPA and DHA were added to DOPC membranes that lacked cholesterol, they had similar effects on membrane K_{app}, reducing the value from 251 mN/m to 205 and 199 mN/m, respectively. The addition of low levels of cholesterol (25 mol%) did not change this general trend. In contrast, when higher levels of cholesterol (45 mol%) were incorporated into DOPC membranes, we observed that EPA and DHA now had different effects on membrane K_{app}, with EPA having a significantly higher K_{app}-value (463 mN/m) than DHA (357 mN/m). This result demonstrates that cholesterol concentration alters the effect of EPA and DHA on the K_{app} of DOPC membranes.

TABLE 4 K_{app}-values of POPC, cholesterol, and fatty acid membranes

	50% chol, 50% POPC	25% OA, 45% chol, 30% POPC	25% EPA, 45% chol, 30% POPC	25% DHA, 45% chol, 30% POPC
K_{app} (mN/m)	545 ± 16	600 ± 24	837 ± 24	462 ± 21
n	27	21	27	33

Sample names indicate lipid stock compositions in chloroform. Values are represented as mean ± SE.

Why might EPA and DHA differentially affect the propensity of a bilayer membrane to stretch when cholesterol is present in high concentrations? Cholesterol can have several effects on the physical properties of membranes that could explain this phenomenon. First, cholesterol increases the packing density of lipid chains and bilayer thickness, leading to increases in the bending rigidity and area expansion modulus of membranes (33,40,67). These effects appear to hold for both saturated as well as unsaturated membranes (68). DHA has one more unsaturated bond than EPA, and differential effects on membrane K_{app} that may not be apparent at low K_{app}-values could become more obvious as the membrane is made stiffer (67). Second, cholesterol promotes phase segregation in model membranes, and DHA and EPA are known to interact differently with phase-segregated domains (11,13,16,18,57,59). Membranes containing ordered and disordered lipids can phase segregate into raft-like (ordered) and non-raft-like (disordered) domains observed in cellular membranes (50,56,69,70). Cholesterol typically associates with raft-like domains but can also induce nanodomain formation when incorporated into membranes containing only one phospholipid, like in POPC or DOPC (49,54,55,71,72). Experiments with model and cell-derived membranes have shown that DHA has highly unfavorable interactions with cholesterol and does not pack into ordered, raft-like phases and instead segregates into disordered domains (11,14,15,18,57,58,73,74). In contrast, EPA and other less-disordered ω-3 fatty acids appear to inhibit or disrupt ordered domains relative to DHA (18,59). These previous results suggest membrane organization may affect membrane K_{app}.

We hypothesize that the differences we observed in K_{app} when membranes contained high levels of cholesterol and either DHA or EPA were, in part, due to differences in molecular interactions between cholesterol and lipid acyl chains. When lipids and cholesterol are more evenly dispersed throughout the membrane, there are increased Van der Waals interactions between phospholipids and cholesterol, which can increase the apparent area expansion modulus, requiring more tension to stretch a membrane (33). In contrast, when cholesterol is sequestered into ordered domains, the net number of cholesterol interactions with phospholipids is reduced (17). In effect, we hypothesize the reduction of K_{app} of DHA-containing membranes, compared to EPA-containing membranes, is due to nonuniform membrane deformation because of reduced interactions between phospholipids and cholesterol when cholesterol is phase segregated. Put another way, it appears that by segregating a molecule (cholesterol) that typically stiffens a membrane, that molecule has less impact on long-range membrane properties than when it is well mixed into the membrane. In summary, we expect cholesterol phase segregation is reduced in the presence of EPA, leading to more cholesterol-lipid interactions and a higher K_{app} in this condition relative to DHA. For membranes with a significant level of cholesterol-rich domains, we hypothesize that in response to applied tension, the majority of membrane stretching occurred in the liquid-disordered phase and deformation was reduced in segregated, stiffer, ordered domains. This effect of nonuniform stretching would explain a net decrease in membrane K_{app} compared to membranes with homogenously distributed cholesterol and lipids (Fig. 4 *B*).

We further observed that we could change lipid-cholesterol interactions by changing the diacyl lipids; by switching the phospholipid from DOPC to POPC, we increased cholesterol-lipid interactions, and the differential effects of EPA and DHA on K_{app} further increased. Differences in K_{app} between membranes constructed from POPC or DOPC and containing high cholesterol concentrations may be explained by the increased content of saturated acyl chains in POPC membranes (Figs. 3 and 4; (40)). This increase in saturation is known to increase the stiffening effect of cholesterol, increasing membrane K_{app} (33). Our results demonstrate that cholesterol concentration (Figs. 2 and 3), and phospholipid identity (Figs. 3 *C* and 4 *A*) can affect how individual fatty acids change membrane K_{app}. These results highlight the potential for variability in lipid composition to affect how a given fatty acid will change membrane biophysical properties (16): if a membrane is fairly elastic, different fatty acids may have small effects on membrane elasticity; however, if a membrane is stiffer, small differences in fatty acid unsaturation and chain length may have significant effects on membrane elasticity.

Our findings also help explain why EPA and DHA may have differential effects on the behavior of membrane proteins. Previous studies have shown that EPA and DHA differentially impact membrane protein activity when the fatty acids were added to cells, but the mechanism was unclear (6,7,19). In these studies, the properties of bending rigidity and viscosity were investigated, which probe the propensity of a membrane to move out of plane or for lipids to move past one another. Both properties were similarly modified by EPA and DHA. In contrast, our study, which explored the propensity of a membrane to stretch in plane, identified differences between EPA- and DHA-containing samples.

Finally, these results contribute to the growing theory that certain changes in protein activity may be due to alterations of the physical membrane environment surrounding the protein rather than distinct chemical binding effects of the fatty acid (5,8,22). FFAs that remodel membranes can alter membrane protein activity in two ways. First, FFAs may be able to alter the concentration of certain lipids around the protein. For example, DHA, which has been shown to shift cholesterol into crystalline nanodomains (18), could soften the local membrane area or reduce hydrophobic thickness through the removal of local cholesterol. This removal of cholesterol and effective softening of a local membrane environment would, in turn, alter the activity of certain channel proteins, most obviously mechanosensitive channels (75–77). Second, membrane remodeling can alter membrane composition through altering the phase in which the protein resides (12,20). Toward this possibility, membrane remodeling has been shown to alter membrane protein domain localization and activity (20,23,51). Both of these potential mechanisms would change the local mechanical properties of the membrane surrounding a protein, affect how much that membrane stretches in response to applied force, and in turn alter protein activity. By influencing the activation, enhancement, or sensitization of ion channel gating, these mechanical changes have the potential to affect a wide range of physiological responses from synaptic plasticity to cognitive functions.

CONCLUSIONS

Here, we demonstrated the effects of various FFAs on DOPC, DOPC/cholesterol, and POPC/cholesterol model membranes. We found that PUFAs generally reduce K_{app} of model membranes. When cholesterol membrane content is high, we found that the PUFAs EPA and DHA exhibit different effects on membrane K_{app}. This result can possibly be explained by the presence of cholesterol crystalline nanodomains, which are expected to be larger in the presence of DHA compared to EPA. This structural difference may alter global membrane force transmission, resulting in our observed differences of membrane K_{app}. Overall, our results demonstrated that FFAs can differentially alter membrane mechanical properties to an extent that can be measured via micropipette aspiration and likely sensed by cellular components, such as membrane proteins, when incorporated into cellular membranes. The mechanistic understanding of the nonspecific modulation of membrane-embedded proteins has the potential to decipher the elusive effects of fatty acids on various membrane proteins and the broader alteration of biological processes.

SUPPORTING MATERIAL

Supporting material can be found online at https://doi.org/10.1016/j.bpj.2021.04.009.

AUTHOR CONTRIBUTIONS

M.L.J., H.A.F., J.A.P., P.M.V., and N.P.K. designed research. M.L.J., H.A.F., and J.A.P. performed research and analyzed data. M.L.J., H.A.F., J.A.P., P.M.V., and N.P.K. wrote the manuscript.

ACKNOWLEDGMENTS

We thank Prof. Robert Raphael for his experimental advice, helpful discussions, and careful reading of the manuscript. We also thank members of the Kamat Lab for thoughtful discussions.

This work was supported by the Air Force Office of Scientific Research YIP FA9550-19-1-0039 P00001 to N.P.K., the Searle Funds at The Chicago Community Trust, and a National Science Foundation (NSF) grant MCB-1935356 (N.P.K.). M.L.J. was supported by Grant No. T32GM008382 from the National Institute of General Medical Sciences and The American Heart Association Predoctoral Fellowship under Grant No. 20PRE35180215. J.A.P. was supported by the NSF Graduate Research Fellowship and the Ryan Fellowship and International Institute for Nanotechnology at Northwestern University. P.M.V. and H.A.F. were supported by NSF grant CMMI-1748049. This work made use of IMSERC at Northwestern University. IMSERC has received support from the Soft and Hybrid Nanotechnology Experimental Resource (NSF ECCS-1542205), the State of Illinois, and the International Institute for Nanotechnology. Wayne State Lipidomics Core Facility is supported in part by National Center for Research Resources, National Institutes of Health Grant S10RR027926.

SUPPORTING CITATIONS

References (78–80) can be found in the Supporting material.

REFERENCES

1. Brassard, P., A. Larbi, …, T. Fülöp. 2007. Modulation of T-cell signalling by non-esterified fatty acids. *Prostaglandins Leukot. Essent. Fatty Acids.* 77:337–343.
2. Kawamoto, J., T. Kurihara, …, N. Esaki. 2009. Eicosapentaenoic acid plays a beneficial role in membrane organization and cell division of a cold-adapted bacterium, Shewanella livingstonensis Ac10. *J. Bacteriol.* 191:632–640.
3. Vásquez, V., M. Krieg, …, M. B. Goodman. 2014. Phospholipids that contain polyunsaturated fatty acids enhance neuronal cell mechanics and touch sensation. *Cell Rep.* 6:70–80.
4. Du, Y., C. G. Taylor, and P. Zahradka. 2019. Modulation of endothelial cell responses and vascular function by dietary fatty acids. *Nutr. Rev.* 77:614–629.
5. Ridone, P., S. L. Grage, …, B. Martinac. 2018. "Force-from-lipids" gating of mechanosensitive channels modulated by PUFAs. *J. Mech. Behav. Biomed. Mater.* 79:158–167.
6. Bruno, M. J., R. E. Koeppe, II, and O. S. Andersen. 2007. Docosahexaenoic acid alters bilayer elastic properties. *Proc. Natl. Acad. Sci. USA.* 104:9638–9643.
7. Carrillo-Tripp, M., and S. E. Feller. 2005. Evidence for a mechanism by which ω-3 polyunsaturated lipids may affect membrane protein function. *Biochemistry.* 44:10164–10169.
8. Cordero-Morales, J. F., and V. Vásquez. 2018. How lipids contribute to ion channel function, a fat perspective on direct and indirect interactions. *Curr. Opin. Struct. Biol.* 51:92–98.
9. Hamilton, J. A., and F. Kamp. 1999. How are free fatty acids transported in membranes? Is it by proteins or by free diffusion through the lipids? *Diabetes.* 48:2255–2269.

10. Olbrich, K., W. Rawicz, …, E. Evans. 2000. Water permeability and mechanical strength of polyunsaturated lipid bilayers. *Biophys. J.* 79:321–327.

11. Levental, K. R., J. H. Lorent, …, I. Levental. 2016. Polyunsaturated lipids regulate membrane domain stability by tuning membrane order. *Biophys. J.* 110:1800–1810.

12. Stillwell, W., and S. R. Wassall. 2003. Docosahexaenoic acid: membrane properties of a unique fatty acid. *Chem. Phys. Lipids.* 126:1–27.

13. Leng, X., J. J. Kinnun, …, S. R. Wassall. 2018. All n-3 PUFA are not the same: MD simulations reveal differences in membrane organization for EPA, DHA and DPA. *Biochim. Biophys. Acta Biomembr.* 1860:1125–1134.

14. Wassall, S. R., and W. Stillwell. 2009. Polyunsaturated fatty acid-cholesterol interactions: domain formation in membranes. *Biochim. Biophys. Acta.* 1788:24–32.

15. Wassall, S. R., and W. Stillwell. 2008. Docosahexaenoic acid domains: the ultimate non-raft membrane domain. *Chem. Phys. Lipids.* 153:57–63.

16. Williams, J. A., S. E. Batten, …, S. R. Wassall. 2012. Docosahexaenoic and eicosapentaenoic acids segregate differently between raft and non-raft domains. *Biophys. J.* 103:228–237.

17. Georgieva, R., C. Chachaty, …, G. Staneva. 2015. Docosahexaenoic acid promotes micron scale liquid-ordered domains. A comparison study of docosahexaenoic versus oleic acid containing phosphatidylcholine in raft-like mixtures. *Biochim. Biophys. Acta.* 1848:1424–1435.

18. Mason, R. P., R. F. Jacob, …, A. Chattopadhyay. 2016. Eicosapentaenoic acid reduces membrane fluidity, inhibits cholesterol domain formation, and normalizes bilayer width in atherosclerotic-like model membranes. *Biochim. Biophys. Acta.* 1858:3131–3140.

19. Romero, L. O., A. E. Massey, …, V. Vásquez. 2019. Dietary fatty acids fine-tune Piezo1 mechanical response. *Nat. Commun.* 10:1200.

20. Javanainen, M., G. Enkavi, …, I. Vattulainen. 2019. Reduced level of docosahexaenoic acid shifts GPCR neuroreceptors to less ordered membrane regions. *PLoS Comput. Biol.* 15:e1007033.

21. Teng, J., S. Loukin, …, C. Kung. 2015. The force-from-lipid (FFL) principle of mechanosensitivity, at large and in elements. *Pflugers Arch.* 467:27–37.

22. Lundbaek, J. A., P. Birn, …, O. S. Andersen. 2004. Regulation of sodium channel function by bilayer elasticity: the importance of hydrophobic coupling. Effects of micelle-forming amphiphiles and cholesterol. *J. Gen. Physiol.* 123:599–621.

23. Caires, R., F. J. Sierra-Valdez, …, J. F. Cordero-Morales. 2017. Omega-3 fatty acids modulate TRPV4 function through plasma membrane remodeling. *Cell Rep.* 21:246–258.

24. Vitkova, V., D. Mitkova, and G. Staneva. 2014. Lyso- and omega-3-containing phosphatidylcholines alter the bending elasticity of lipid membranes. *Colloids Surf. A Physicochem. Eng. Asp.* 460:191–195.

25. Georgieva, R., K. Mircheva, …, G. Staneva. 2016. Phospholipase A2-induced remodeling processes on liquid-ordered/liquid-disordered membranes containing docosahexaenoic or oleic acid: a comparison study. *Langmuir.* 32:1756–1770.

26. Evans, E. A., R. Waugh, and L. Melnik. 1976. Elastic area compressibility modulus of red cell membrane. *Biophys. J.* 16:585–595.

27. Wiggins, P., and R. Phillips. 2005. Membrane-protein interactions in mechanosensitive channels. *Biophys. J.* 88:880–902.

28. Nakayama, Y., K. Komazawa, …, B. Martinac. 2018. Evolutionary specialization of MscCG, an MscS-like mechanosensitive channel, in amino acid transport in Corynebacterium glutamicum. *Sci. Rep.* 8:12893.

29. Rawicz, W., K. C. Olbrich, …, E. Evans. 2000. Effect of chain length and unsaturation on elasticity of lipid bilayers. *Biophys. J.* 79:328–339.

30. Zhou, Y., and R. M. Raphael. 2005. Effect of salicylate on the elasticity, bending stiffness, and strength of SOPC membranes. *Biophys. J.* 89:1789–1801.

31. Jacobs, M. L., M. A. Boyd, and N. P. Kamat. 2019. Diblock copolymers enhance folding of a mechanosensitive membrane protein during cell-free expression. *Proc. Natl. Acad. Sci. USA.* 116:4031–4036.

32. Jin, L., N. P. Kamat, …, J. W. Szostak. 2018. Fatty acid/phospholipid blended membranes: a potential intermediate state in protocellular evolution. *Small.* 14:e1704077.

33. Rawicz, W., B. A. Smith, …, E. Evans. 2008. Elasticity, strength, and water permeability of bilayers that contain raft microdomain-forming lipids. *Biophys. J.* 94:4725–4736.

34. Kamat, N. P., M. H. Lee, …, D. A. Hammer. 2011. Micropipette aspiration of double emulsion-templated polymersomes. *Soft Matter.* 7:9863–9866.

35. Simard, J. R., F. Kamp, and J. A. Hamilton. 2008. Measuring the adsorption of fatty acids to phospholipid vesicles by multiple fluorescence probes. *Biophys. J.* 94:4493–4503.

36. Høyrup, P., J. Davidsen, and K. Jørgensen. 2001. Lipid membrane partitioning of lysolipids and fatty acids: effects of membrane phase structure and detergent chain length. *J. Phys. Chem. B.* 105:2649–2657.

37. Roy, A., R. Dutta, …, N. Sarkar. 2016. A comparative study of the influence of sugars sucrose, trehalose, and maltose on the hydration and diffusion of DMPC lipid bilayer at complete hydration: investigation of structural and spectroscopic aspect of lipid-sugar interaction. *Langmuir.* 32:5124–5134.

38. Schindelin, J., I. Arganda-Carreras, …, A. Cardona. 2012. Fiji: an open-source platform for biological-image analysis. *Nat. Methods.* 9:676–682.

39. Fricke, K., and E. Sackmann. 1984. Variation of frequency spectrum of the erythrocyte flickering caused by aging, osmolarity, temperature and pathological changes. *Biochim. Biophys. Acta.* 803:145–152.

40. Gracià, R. S., N. Bezlyepkina, …, R. Dimova. 2010. Effect of cholesterol on the rigidity of saturated and unsaturated membranes: fluctuation and electrodeformation analysis of giant vesicles. *Soft Matter.* 6:1472–1482.

41. Henriksen, J. R., and J. H. Ipsen. 2002. Thermal undulations of quasi-spherical vesicles stabilized by gravity. *Eur Phys J E Soft Matter.* 9:365–374.

42. Faizi, H. A., C. J. Reeves, …, R. Dimova. 2020. Fluctuation spectroscopy of giant unilamellar vesicles using confocal and phase contrast microscopy. *Soft Matter.* 16:8996–9001.

43. Rautu, S. A., D. Orsi, …, M. S. Turner. 2017. The role of optical projection in the analysis of membrane fluctuations. *Soft Matter.* 13:3480–3483.

44. Faizi, H. A., S. L. Frey, …, P. M. Vlahovska. 2019. Bending rigidity of charged lipid bilayer membranes. *Soft Matter.* 15:6006–6013.

45. Tyler, A. I. I., J. L. Greenfield, …, S. Purushothaman. 2019. Coupling phase behavior of fatty acid containing membranes to membrane biomechanics. *Front. Cell Dev. Biol.* 7:187.

46. Zhou, Y., C. K. Berry, …, R. M. Raphael. 2007. Peroxidation of polyunsaturated phosphatidyl-choline lipids during electroformation. *Biomaterials.* 28:1298–1306.

47. Koenig, B. W., H. H. Strey, and K. Gawrisch. 1997. Membrane lateral compressibility determined by NMR and x-ray diffraction: effect of acyl chain polyunsaturation. *Biophys. J.* 73:1954–1966.

48. Yang, X., W. Sheng, …, J. C.-M. Lee. 2011. Effects of fatty acid unsaturation numbers on membrane fluidity and α-secretase-dependent amyloid precursor protein processing. *Neurochem. Int.* 58:321–329.

49. Tulenko, T. N., M. Chen, …, R. P. Mason. 1998. Physical effects of cholesterol on arterial smooth muscle membranes: evidence of immiscible cholesterol domains and alterations in bilayer width during atherogenesis. *J. Lipid Res.* 39:947–956.

50. Schroeder, F., J. K. Woodford, …, C. Joiner. 1995. Cholesterol domains in biological membranes. *Mol. Membr. Biol.* 12:113–119.

51. Ridone, P., E. Pandzic, …, B. Martinac. 2020. Disruption of membrane cholesterol organization impairs the activity of PIEZO1 channel clusters. *J. Gen. Physiol.* 152:e201912515.

52. McIntosh, T. J., A. Vidal, and S. A. Simon. 2003. Sorting of lipids and transmembrane peptides between detergent-soluble bilayers and detergent-resistant rafts. *Biophys. J.* 85:1656–1666.

53. Sherratt, S. C. R., and R. P. Mason. 2018. Eicosapentaenoic acid and docosahexaenoic acid have distinct membrane locations and lipid interactions as determined by x-ray diffraction. *Chem. Phys. Lipids.* 212:73–79.

54. Suga, K., and H. Umakoshi. 2013. Detection of nanosized ordered domains in DOPC/DPPC and DOPC/Ch binary lipid mixture systems of large unilamellar vesicles using a TEMPO quenching method. *Langmuir.* 29:4830–4838.

55. Javanainen, M., H. Martinez-Seara, and I. Vattulainen. 2017. Nanoscale membrane domain formation driven by cholesterol. *Sci. Rep.* 7:1143.

56. Duraisamy, Y., D. Lambert, …, P. J. Padfield. 2007. Differential incorporation of docosahexaenoic acid into distinct cholesterol-rich membrane raft domains. *Biochem. Biophys. Res. Commun.* 360:885–890.

57. Kinnun, J. J., R. Bittman, …, S. R. Wassall. 2018. DHA modifies the size and composition of raftlike domains: a solid-state ^{2}H NMR study. *Biophys. J.* 114:380–391.

58. Shaikh, S. R., M. R. Brzustowicz, …, S. R. Wassall. 2002. Monounsaturated PE does not phase-separate from the lipid raft molecules sphingomyelin and cholesterol: role for polyunsaturation? *Biochemistry.* 41:10593–10602.

59. Lin, X., J. H. Lorent, …, I. Levental. 2016. Domain stability in biomimetic membranes driven by lipid polyunsaturation. *J. Phys. Chem. B.* 120:11930–11941.

60. Tierney, K. J., D. E. Block, and M. L. Longo. 2005. Elasticity and phase behavior of DPPC membrane modulated by cholesterol, ergosterol, and ethanol. *Biophys. J.* 89:2481–2493.

61. Stevens, M. M., A. R. Honerkamp-Smith, and S. L. Keller. 2010. Solubility limits of cholesterol, lanosterol, ergosterol, stigmasterol, and β-sitosterol in electroformed lipid vesicles. *Soft Matter.* 6:5882–5890.

62. Portet, T., S. E. Gordon, and S. L. Keller. 2012. Increasing membrane tension decreases miscibility temperatures; an experimental demonstration via micropipette aspiration. *Biophys. J.* 103:L35–L37.

63. Pan, J., S. Tristram-Nagle, and J. F. Nagle. 2009. Effect of cholesterol on structural and mechanical properties of membranes depends on lipid chain saturation. *Phys. Rev. E Stat. Nonlin. Soft Matter Phys.* 80:021931.

64. Hilburger, C. E., M. L. Jacobs, …, N. P. Kamat. 2019. Controlling secretion in artificial cells with a membrane and gate. *ACS Synth. Biol.* 8:1224–1230.

65. Revskij, D., S. Haubold, …, M. Mielenz. 2019. Dietary fatty acids affect red blood cell membrane composition and red blood cell ATP release in dairy cows. *Int. J. Mol. Sci.* 20:2769.

66. Bryk, A. H., and J. R. Wiśniewski. 2017. Quantitative analysis of human red blood cell proteome. *J. Proteome Res.* 16:2752–2761.

67. Smaby, J. M., M. M. Momsen, …, R. E. Brown. 1997. Phosphatidylcholine acyl unsaturation modulates the decrease in interfacial elasticity induced by cholesterol. *Biophys. J.* 73:1492–1505.

68. Chakraborty, S., M. Doktorova, …, R. Ashkar. 2020. How cholesterol stiffens unsaturated lipid membranes. *Proc. Natl. Acad. Sci. USA.* 117:21896–21905.

69. Owen, D. M., M. A. A. Neil, …, A. I. Magee. 2007. Optical techniques for imaging membrane lipid microdomains in living cells. *Semin. Cell Dev. Biol.* 18:591–598.

70. Li, G., Q. Wang, …, E. London. 2020. Nanodomains can persist at physiologic temperature in plasma membrane vesicles and be modulated by altering cell lipids. *J. Lipid Res.* 61:758–766.

71. Armstrong, C. L., D. Marquardt, …, M. C. Rheinstädter. 2013. The observation of highly ordered domains in membranes with cholesterol. *PLoS One.* 8:e66162.

72. Barrett, M. A., S. Zheng, …, M. C. Rheinstädter. 2013. Solubility of cholesterol in lipid membranes and the formation of immiscible cholesterol plaques at high cholesterol concentrations. *Soft Matter.* 9:9342–9351.

73. Soni, S. P., D. S. LoCascio, …, S. R. Wassall. 2008. Docosahexaenoic acid enhances segregation of lipids between raft and nonraft domains: ^{2}H-NMR study. *Biophys. J.* 95:203–214.

74. Shaikh, S. R., D. S. Locascio, …, W. Stillwell. 2009. Oleic- and docosahexaenoic acid-containing phosphatidylethanolamines differentially phase separate from sphingomyelin. *Biochim. Biophys. Acta.* 1788:2421–2426.

75. Xue, F., C. D. Cox, …, B. Martinac. 2020. Membrane stiffness is one of the key determinants of *E. coli* MscS channel mechanosensitivity. *Biochim. Biophys. Acta Biomembr.* 1862:183203.

76. Rajagopalan, L., J. N. Greeson, …, W. E. Brownell. 2007. Tuning of the outer hair cell motor by membrane cholesterol. *J. Biol. Chem.* 282:36659–36670.

77. Kamar, R. I., L. E. Organ-Darling, and R. M. Raphael. 2012. Membrane cholesterol strongly influences confined diffusion of prestin. *Biophys. J.* 103:1627–1636.

78. Peruzzi, J. A., M. L. Jacobs, …, N. P. Kamat. 2019. Barcoding biological reactions with DNA-functionalized vesicles. *Angew. Chem. Int. Ed. Engl.* 58:18683–18690.

79. Onuki, Y., M. Morishita, …, K. Takayama. 2006. Docosahexaenoic acid and eicosapentaenoic acid induce changes in the physical properties of a lipid bilayer model membrane. *Chem. Pharm. Bull. (Tokyo).* 54:68–71.

80. Dimova, R. 2014. Recent developments in the field of bending rigidity measurements on membranes. *Adv. Colloid Interface Sci.* 208:225–234.

Biophysical Journal, Volume *120*

Supplemental information

EPA and DHA differentially modulate membrane elasticity in the presence of cholesterol

Miranda L. Jacobs, Hammad A. Faizi, Justin A. Peruzzi, Petia M. Vlahovska, and Neha P. Kamat

TABLE OF CONTENTS

SUPPORTING METHODS

Materials

Lipid peroxidation (MDA) assay, 1,6-diphenyl-1,3,5-hexatriene (DPH), and dipyrromethene boron difluoride cholesterol (BODIPY-cholesterol) were purchased from Millipore Sigma (St. Louis, MO). Triton X-100, Nonesterified fatty acid (NEFA HR-2) and Phospholipids-C Fujifilm quantitation kits were purchased from Thermo Fisher Scientific (Waltham, MA).

Differential scanning calorimetry

Differential scanning calorimetry was performed to determine the phase transition temperature of vesicles using a Mettler Toledo Polymer DSC measurement system (1). Vesicles were prepared using thin film hydration methods and extruded to 100 nm using a mini-extruder (Avanti Polar Lipids (Alabaster, AL)). 30 μL of 20 mM vesicles in water were sealed into an aluminum pan. Scans were performed from -40 to 60ºC with a ramp rate of 10 °K/min under helium gas. Phase transition temperatures were determined using the Mettler STARe analysis software's glass transition tool.

Fluorescence Anisotropy

Membrane anisotropy measurements were performed as described previously (2). 0.5 mM small unilamellar vesicles prepared in 300 mOsm PBS containing 0.2 mol% DPH and various compositions of DOPC, fatty acid, and cholesterol, were analyzed using an Agilent Technologies Cary Eclipse Fluorescence Spectrophotometer with the Automated Polarization Accessory. Fluorescence anisotropy of DPH was assessed at the following excitation and emission wavelengths: 360 nm and 435 nm. Fluorescence anisotropy (r) was calculated automatically by software provided with the instrument, according to $r = (I_{vv} - I_{vh}G) / (I_{vv} + 2I_{vh}G)$, where I_{vv} and I_{vh} are the intensities of the vertically and horizontally polarized components of the fluorescent light, respectively, after excitation with vertically polarized light. $G = I_{hv}/I_{hh}$ is a grating correction factor for the optical system.

Fatty acid oxidation assays

Lipid oxidation levels were determined of electroformed samples. The detection of conjugated dienes was performed as described previously (3). Immediately following electroformation, 50 μL of electroformed vesicles were diluted in pure ethanol to 1 mL. Oxidized positive controls were created by heating electroformed samples at 60 °C for 48 hours. Absorbance was measured at 230 nm using a Cary Eclipse spectrophotometer and values were normalized to pure, unoxidized DOPC.

Fatty acid membrane composition assays

Fatty acid incorporation into electroformed GUVs was determined as described previously (4) using a Fujifilm non-esterified fatty acid (NEFA) and phospholipid quantitation kit. Vesicles constructed using electroformation techniques were diluted in PBS to bring the fatty acid concentration below the CMC of oleic acid (5) to facilitate maximal partitioning of fatty acid into the bilayer and to mimic our micropipette aspiration study conditions (4). We then centrifuged our vesicles at 21,000xg for 30 min to pellet the vesicles. The supernatant was discarded to remove unincorporated fatty acids and the vesicle pellet was resuspended in PBS. We then disrupted the bilayer structure using 1% Triton X-100 and divided each sample into two. We incubated our samples with each kit activation reagent and measured non-esterified fatty acid and phospholipid concentrations in our vesicles using absorbance at 550 and 600 nm, respectively. We constructed standard curves of fatty acids from 0.03 – 1.25 mM and phospholipids from 0 – 10 mM and measured absorbance at 550 and 600 nm, respectively after incubating with each kit activation reagent. Fatty acid and phospholipid sample concentrations were determined using these standard curves and molar ratios were calculated using [FA] / [phospholipid]. Mol% fatty acid was determined in binary mixtures of POPC and fatty acid by [FA] / ([FA] + [phospholipid]).

Cholesterol distribution determination

The cholesterol distribution in ternary mixtures of POPC, cholesterol and fatty acids were performed using BODIPY-cholesterol fluorescence microscopy. 0.5 mol% BODIPY-cholesterol was incorporated into lipid stocks containing 30 mol% POPC, 45 mol% cholesterol, and 25 mol% OA, EPA, or DHA. Vesicles were formed using electroformation and were immediately imaged using DIC phase-contrast and epifluorescence using a GFP filter set. To determine if cholesterol incorporates at similar amounts in the presence of different fatty acids, the fluorescence intensity in the membranes of GUVs was measured and quantified using Nikon eclipse software. Additionally, to determine if cholesterol was evenly distributed between different vesicles within each sample, fields containing multiple vesicles were imaged using phase-contrast and BODIPY-cholesterol fluorescence.

FRET Domain Disruption Assay

Fatty acid uptake and domain mixing measured to determine phase behavior of cholesterol-containing bilayers. Previous studies have demonstrated that fatty acid treatment leads to relatively even uptake of each fatty acid (4). Therefore, by inserting fatty acids into bilayers containing cholesterol domains, the phase behavior can be observed by a change in dye behavior. Briefly, Membranes containing 18:1 NBD-PE and 18:1 Liss-Rhod PE were used to determine surface area of L_d domains. 0.5, 1, 2, and 3 μL of 100 mM non-esterified fatty acid dissolved in ethanol was added to 100 μL 10 mM 50 mol% DOPC, 50 mol% cholesterol SUVs containing 0.1 mol% total fluorophore, prepared in 300 mOsm PBS, pH 7.4. Bulk Forster Resonance Energy Transfer (FRET) ratios were measured in a Molecular Devices Spectra Max i3 plate reader. 18:1 NBD PE (donor) and 18:1 Liss-Rhod PE (acceptor) fluorescence were excited using 463 nm light and the emission was measured at 517 nm (to determine f_{don}) and 590nm (to determine $F_{acceptor}$) respectively. FRET ratio is defined at f_{don}/f_{acc}. Using a standard curve of mol% dye vs. FRET ratio, relative

changes in surface area available to the dyes can be quantified by first calculating the local mol% dye. Then, a ratio of local mol% dye in untreated over FA-treated vesicle determines the local surface area available to the FRET dyes. When incubated with fatty acids, a large increase in surface area is expected when cholesterol domains are disrupted due to the homogenous dye content rather than being isolated to L_d domains.

Lipidomics Sample Preparation and Analysis

Lipidomic analysis was performed to determine membrane compositions during micropipette aspiration studies. Giant Unilamelar Vesicles (GUVs) were prepared using identical methods to GUVs prepared for micropipette aspiration. GUVs were purified by diluting below the CMC of the fatty acids. Samples were flash frozen in glass vials and stored at -80 °C prior to mass spectrometry. Lipidomic analysis and quantification was performed by the Lipidomics Core Facility at Wayne State University to quantify the amount of phospholipid, cholesterol, and non-esterified fatty acid in each sample. Liquid chromatography-mass (LC-MS) spectrometry was used to quantify these molecules. DOPC and POPC were quantified relative to DPPC-d62 standard, cholesterol was quantified relative to cholesterol-d7 standard, oleic acid was quantified relative to oleic acid-d17, EPA and DHA were quantified relative to arachidonic acid-d8, DHA oxidation was quantified relative to 15-HETE-d8 to measure a range of DHA oxidation analytes X-hydroxy-5E,7Z,10Z,13Z,16Z,19Z-docosahexaenoic acid (4-HDoHE, 7-HDoHE 8-HDoHE 10-HDoHE 11-HDoHE 13-HDoHE 14-HDoHE 16-HDoHE 17-HDoHE 20-HDoHE) and X-hydroperoxy-(4Z,7Z,11E,13Z,16Z,19Z)-docosahexaenoic acid (4-HpDoHE 7-HpDoHE 8-HpDoHE 10-HpDoHE 11-HpDoHE 13-HpDoHE 14-HpDoHE 16-HpDoHE 17-HpDoHE 20-HpDoHE) and the total amount of analyte detected was used to quantify %DHA oxidation. The mol % of phospholipids, fatty acids, and cholesterol were determined from the concentrations of each component calculated via LC-MS and are reported in Table S1.

SUPPORTING TABLES

Table S1. Lipidomic analysis quantifies membrane compositions used for micropipette aspiration. Giant vesicles were prepared and purified using centrifugation to remove unincorporated amphiphiles. Samples were analyzed by liquid chromatography-mass spectrometry (LC-MS). In the absence of cholesterol, all fatty acids included at 25 mol% in chloroform mixtures with lipids subsequently incorporate similarly into DOPC vesicles (to a final concentration of ~6-8 mol %). Additionally, POPC/ cholesterol/ FA mixed at a ratio of 30: 45: 25 mol % in chloroform also exhibited similar incorporation of each polyunsaturated fatty acid (~ 3 mol %) as well as cholesterol (~10 mol%). Various possible DHA oxidation metabolites were quantified and the total mass of metabolites and the total amount of DHA present in the final sample were used to calculate % DHA oxidation. Nm indicates samples were not measured.

DOPC/FA samples	phospholipid mol%	cholesterol mol%	fatty acid mol%	% DHA oxidation
DOPC/ OA	93.5	0.0	6.5	nm
DOPC/ EPA	94.0	0.0	6.0	nm
DOPC/ DHA	92.3	0.0	7.7	0.3

POPC/high chol/FA samples	phospholipid mol%	cholesterol mol%	fatty acid mol%	% DHA oxidation
POPC/ chol	92.9	7.1	0.0	nm
POPC/ chol/ OA	82.1	10.3	7.7	nm
POPC/ chol/ EPA	86.0	11.1	2.9	nm
POPC/ chol/ DHA	84.7	11.7	3.5	0.6

Table S2. Comparison of phase transition temperatures for vesicles composed of DOPC and 1:1 DOPC and cholesterol. The phase transition temperature remains well below ambient temperature, where experiments were carried out. The addition of cholesterol decreases the phase transition temperature.

Sample	$T_{transition}$ (^oC)
2 DOPC : 0 Chol	*-18.89*
1 DOPC : 1 Chol	*-20.96*

Table S3. Comparison of k_c measurements obtained by the flickering spectroscopy method and micropipette aspiration. We compared k_c measurements from select samples using the flickering spectroscopy method and micropipette aspiration in the low-tension regime. We found that the flickering spectroscopy method was more sensitive (6), likely because micropipette aspiration utilizes membrane stretching to determine k_c while flickering spectroscopy does not use external membrane perturbation but both methods produced similar results. We chose to use the flickering spectroscopy method for the majority of our compositions for this reason.

	Micropipette aspiration k_c (k_BT)	**Flickering spectroscopy (k_BT)**
DOPC/ high cholesterol	30.4 +/- 5.5	30.4 +/- 2.6
POPC/ high cholesterol	64.0 +/- 25	60.5 +/- 5.4
DOPC/ high cholesterol/ DHA	27.0 +/- 9.9	37.6 +/- 3.2
DOPC/ high cholesterol/ EPA	40.7 +/- 18.9	33.4 +/- 4.3
DOPC/ high cholesterol/ OA	50.4 +/- 13	20.8 +/- 2.1

SUPPORTING FIGURES

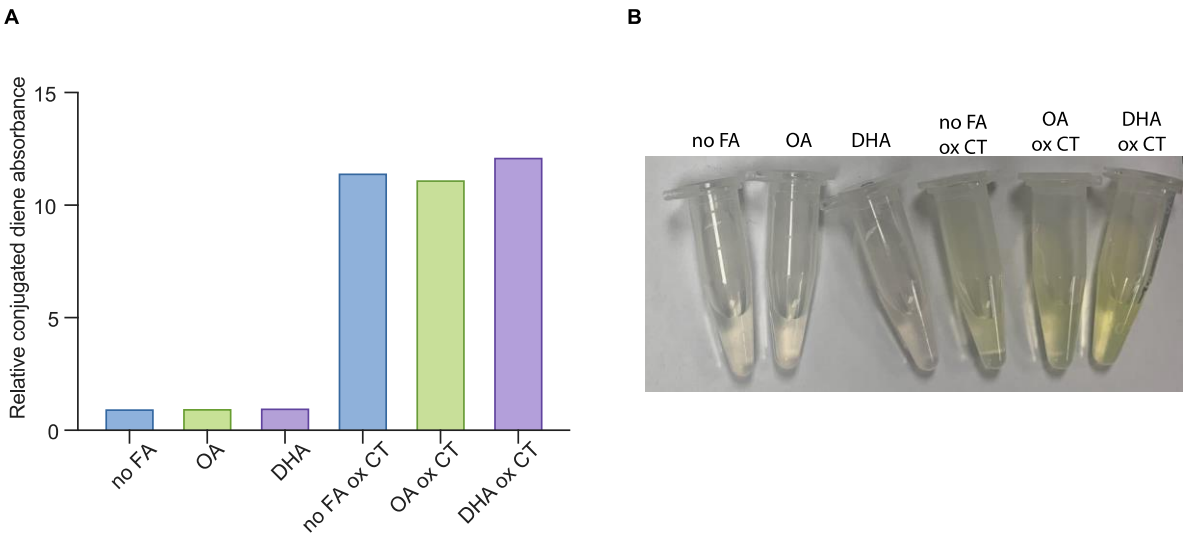

Supplemental Figure S1: Spectroscopic analysis of fatty acid oxidation. Fatty acid oxidation is minimal for PUFAs in our experimental conditions. A) Fatty acid oxidation, measured by conjugated diene presence, is low after electroformation. Immediately following electroformation, conjugated dienes were detected in samples containing only DOPC (no FA), 75 mol% DOPC/ 25 mol% OA (OA), and 75 mol% DOPC/ 25 mol% DHA (DHA) using absorbance at 230 nm in ethanol. Relative conjugated diene absorbance is reported with values normalized to DOPC, as DOPC is expected to be the most resistant to oxidation. We found that minimal oxidation occurred compared to samples subject to extreme heat and high levels of oxidation (ox CT). B) GUV samples are colorless after electroformation. Samples were photographed to demonstrate that they remained clear indicating that electroformed samples are minimally oxidized compared to oxidized samples which were brown.

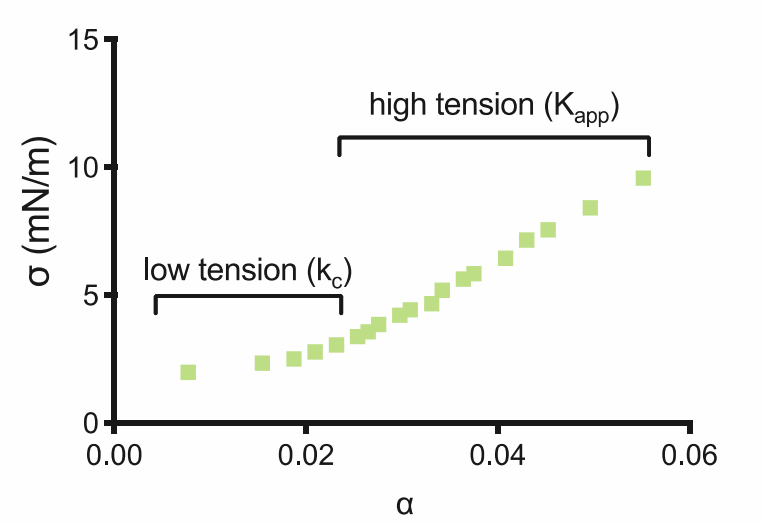

Supplemental Figure S2: Sample micropipette aspiration stress/ strain curve. Micropipette aspiration involves aspirating a vesicle at small intervals ~2 cm H_2O and observing a change in area within the pipette tip. K_{app} is calculated from the rate of change of the stress (σ) (equation S1) and the strain (α) (equation S2) in the high-tension regime, or the slope of this line.

$$\sigma = \frac{\Delta P * R_v * R_p}{R_v - R_p} \text{ (mN/m or dyne/cm)} \quad \text{(S1)}$$

$$\alpha = \frac{\Delta A}{A(o)} \text{ (unitless)} \quad \text{(S2)}$$

Where ΔP is the change in pipette pressure, and R_v and R_p are the vesicle and pipette radius, respectively. ΔA is change in vesicle area within the pipette, A(o) refers to the original vesicle area within the pipette.

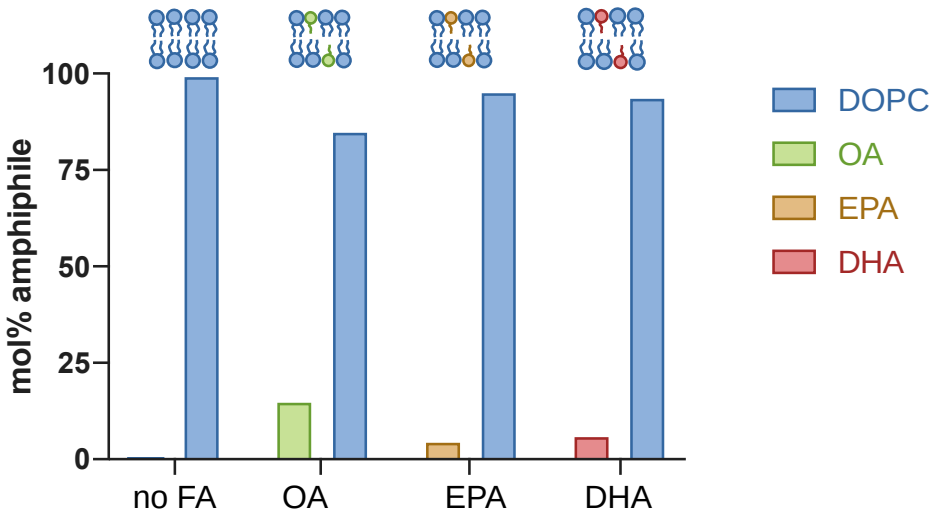

Supplemental Figure S3: Fatty acid incorporation amounts differ based on fatty acid identity. In order to confirm our membrane compositions after electroformation, we measured FA integration using phospholipid and fatty acid quantification kits. We mixed stock solutions containing 25 mol% fatty acid and 75 mol% DOPC in chloroform and created lipid films by removing solvent. The films were rehydrated in 300 mOsm sucrose and were subjected to electroformation to form GUVs. After electroformation, we diluted our GUVs below the fatty acid critical micelle concentration in PBS, pH 7.4, to mimic our micropipette aspiration conditions. We removed unincorporated fatty acids by centrifuging and removing the supernatant and measured the concentration of each class of amphiphile. As a control, we analyzed samples containing pure DOPC, which were found to not contain any fatty acids. We chose to analyze oleic acid (OA), eicosapentaenoic acid (EPA), and docosahexaenoic acid (DHA) because we focus the majority of our studies on these three fatty acids. We found that OA was present at 15 mol% while EPA and DHA were present at 5 mol%.

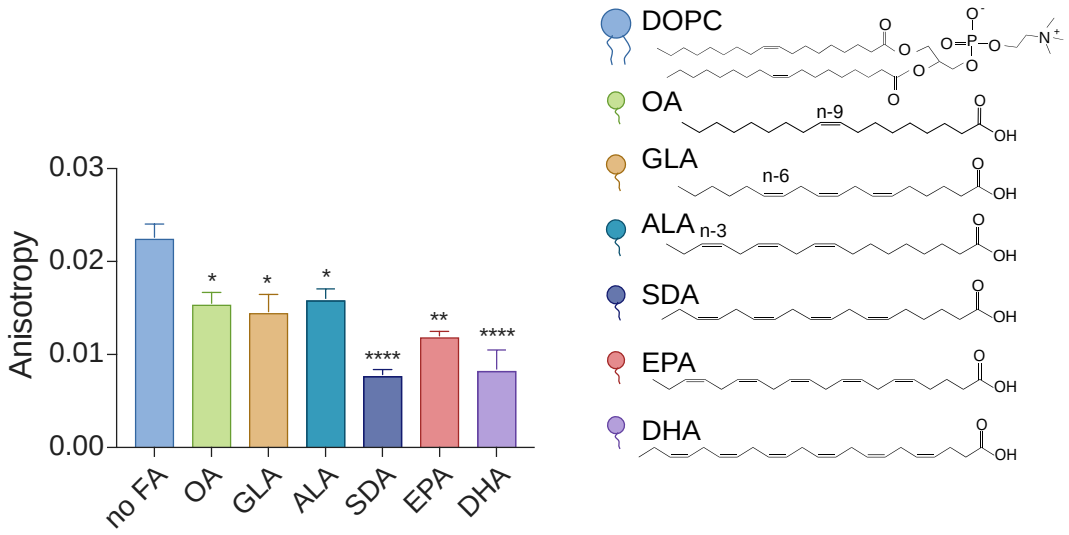

Supplemental Figure S4: Fatty acids increase membrane fluidity. Anisotropy studies were conducted with DOPC vesicles constructed from lipid stocks containing 25 mol% fatty acid and 0.2 mol% 1,6-Diphenyl-1,3,5-hexatriene (DPH) in 300 mOsm PBS, pH 7.4. n=3, P-values were generated by ANOVA using Dunnett's multiple comparisons test compared to no FA. **** $p \leq 0.0001$, ** $p \leq 0.01$, * $p \leq 0.05$, non-significant (ns) $p > 0.5$. Error bars represent standard error of the mean.

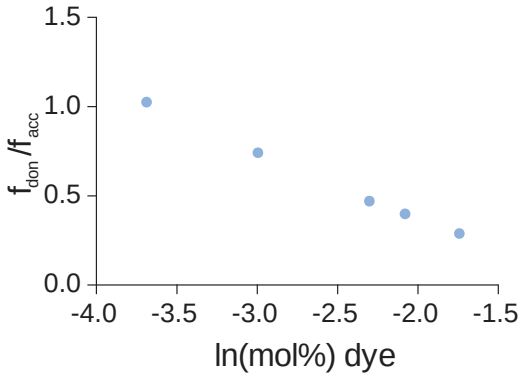

Supplemental Figure S5: FRET standard curve used to calculate relative surface area changes in vesicles. Increasing concentrations of equimolar 18:1 NBD PE and 18:1 Liss Rhod PE were added to 10 mM DOPC vesicles. The FRET ratio (f_{don}/f_{acc}) demonstrates the energy transfer efficiency of the dyes at different concentrations. FRET studies were conducted in PBS, pH 7.4.

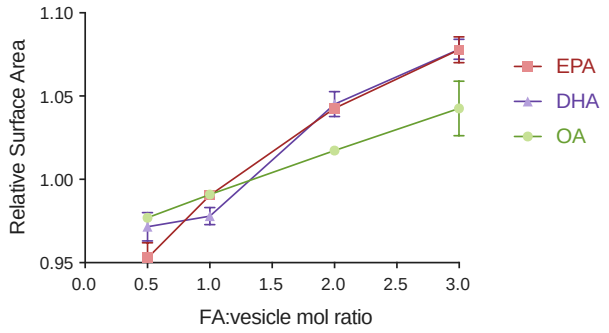

Supplemental Figure S6: In the absence of domains, EPA and DHA affect vesicle surface area similarly. When EPA and DHA are added to 25 mol% chol, 75 mol% DOPC vesicles, EPA and DHA exhibit similar changes in vesicle surface area, unlike vesicles that exhibit phase behavior (Fig 3C). Vesicles were prepared with different concentrations of equimolar 18:1 NBD PE and 18:1 Liss Rhod PE. The FRET ratio (f_{don}/f_{acc}) is used to measure energy transfer efficiency between the dyes after fatty acid addition. n=3, FRET studies were conducted in in 300 mOsm PBS, pH 7.4. Error bars represent standard error of the mean.

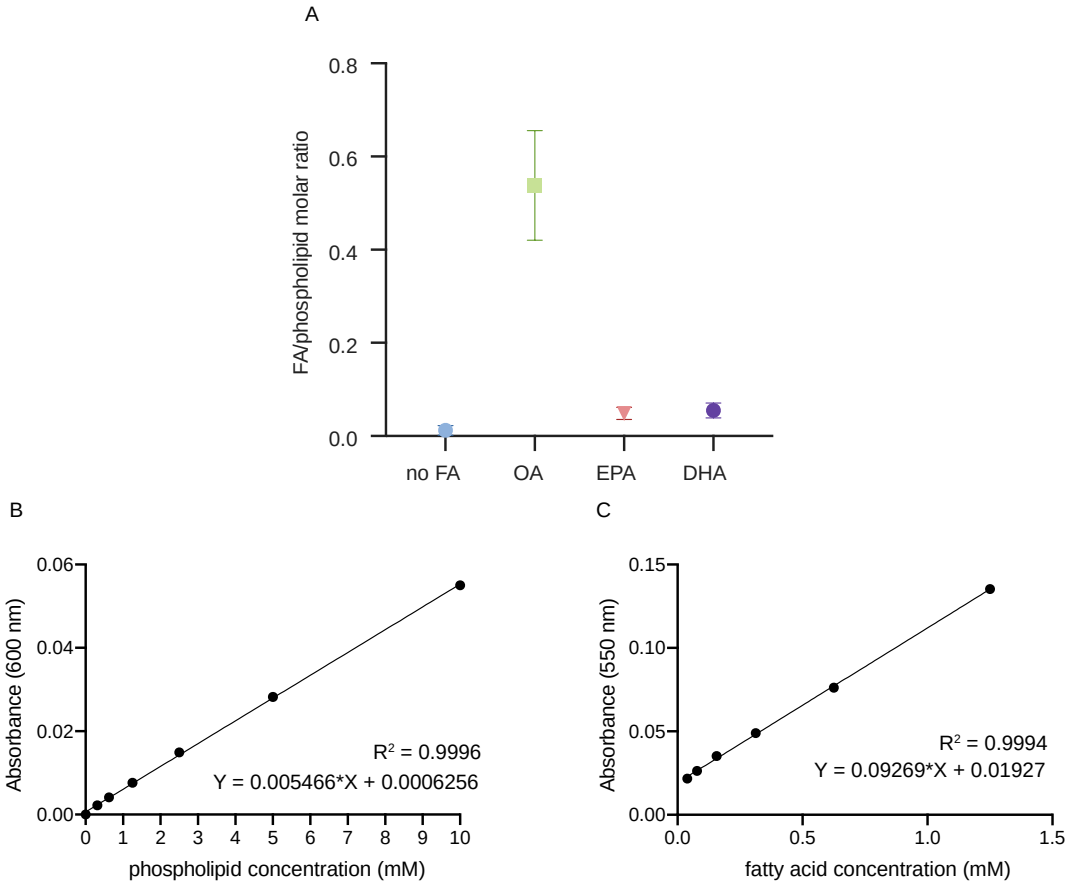

Supplemental Figure S7: Determination of membrane fatty acid composition in ternary mixtures with POPC and cholesterol. A) In order to confirm our membrane compositions of ternary mixtures of membranes constructed from lipid stocks containing 30 mol% POPC, 45 mol% cholesterol, and 25 mol% fatty acid, we used a phospholipid and a fatty acid quantitation kit to determine the mol% of each component. Molar ratios were calculated by dividing the concentration of fatty acid by the phospholipid concentration. POPC and cholesterol only (no FA) demonstrates the specificity of the free fatty acid kit to not detect phospholipids or cholesterol. OA, EPA, and DHA represent samples prepared from stocks containing 25 mol% of each respective fatty acid. Fatty acid and phospholipid concentrations were calculated from standard curves of phospholipid (B), and oleic acid (C).

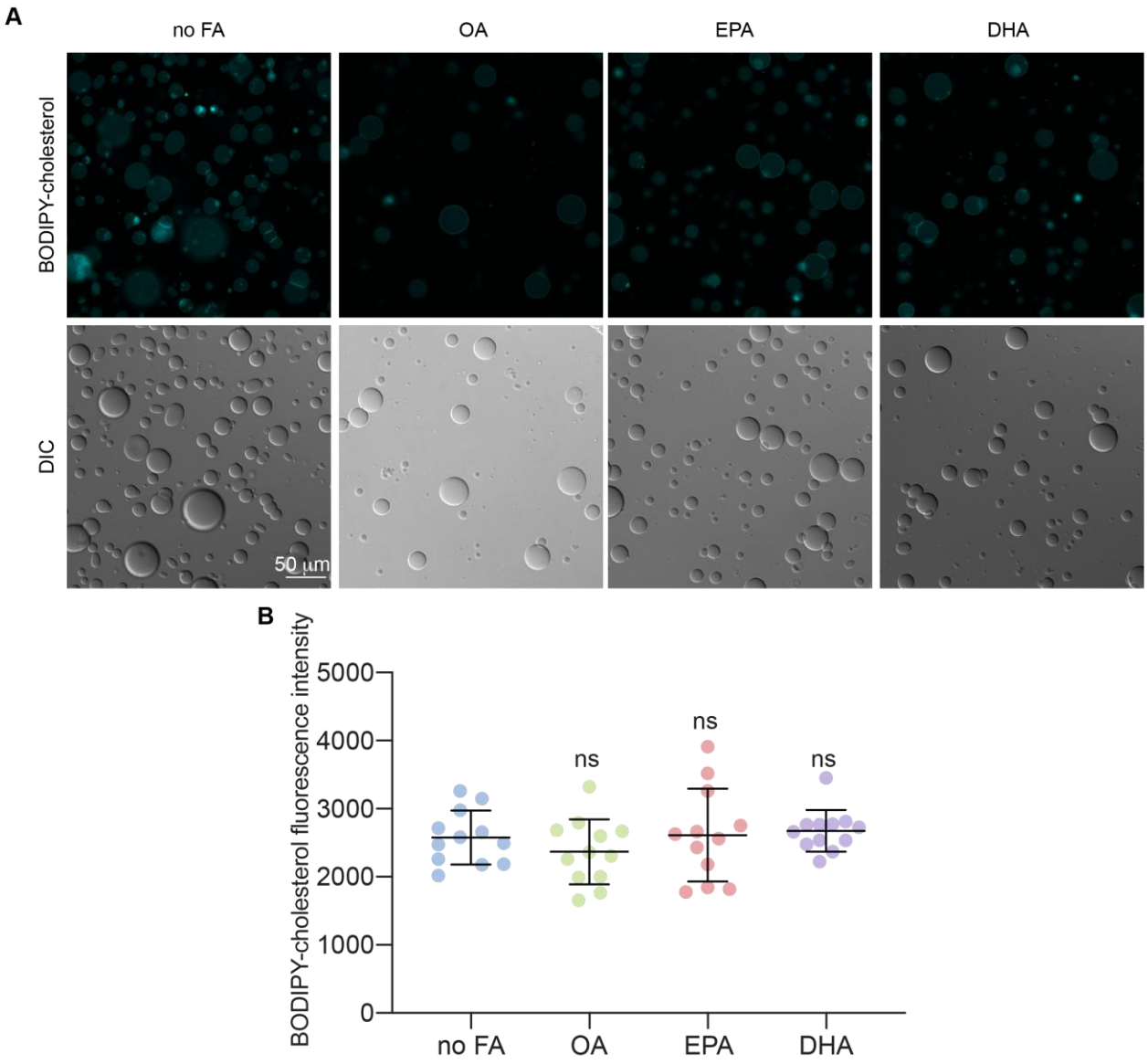

Supplemental Figure S8: Cholesterol is similarly incorporated into membranes containing different fatty acids. A) BODIPY-cholesterol images demonstrate similar incorporation of cholesterol in vesicle populations. BODIPY-cholesterol was incorporated into 30 mol% POPC, 45 mol% cholesterol, 25 mol% fatty acid lipid stocks and GUVs were formed using electroformation techniques. Epifluorescence images are false-colored in cyan and show BODIPY-cholesterol fluorescence at the membrane of all vesicles containing either no FA, OA, EPA, or DHA, scale bar = 50 μm. B) BODIPY-cholesterol fluorescence intensity values reveal no significant difference in cholesterol incorporation between membrane compositions. BODIPY-chol membrane fluorescence was calculated for 12 defect-free vesicles in each population and reported as single values. The center black line indicates mean fluorescence intensity. Error bars represent standard deviation, n=12. P values were generated by ANOVA using Dunnett's multiple comparisons test compared to no FA, non-significant (ns) $P > 0.5$.

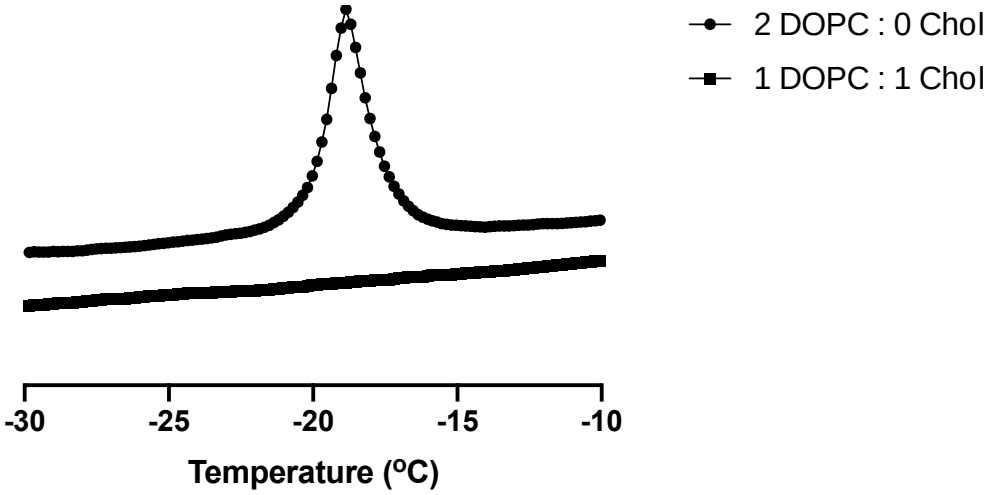

Supplemental Figure S9. Melting temperature of membranes is below ambient temperature and a phase transition is not expected during aspiration measurements (Table S1). DSC thermogram for pure DOPC (2 DOPC: 0 chol) and 50 mol% chol, 50 mol% DOPC (1 DOPC: 1 chol) vesicles. Curves have been corrected using a water control.

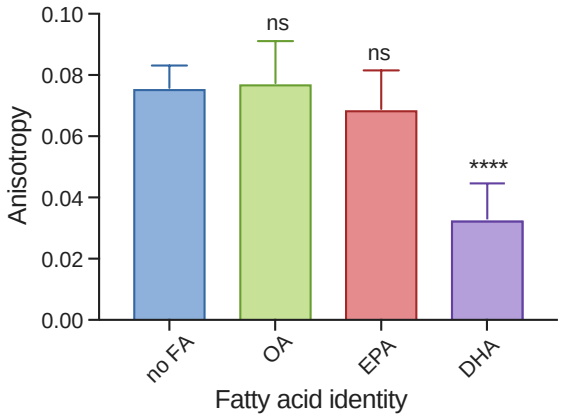

Supplemental Figure S10: DHA increases the fluidity of membranes containing cholesterol. Decreased fluorescence anisotropy occurs with increased membrane fluidity as observed in membranes containing DHA. Anisotropy studies were conducted with vesicles constructed from lipid stocks containing 50 mol% chol, 50 mol% DOPC (no FA) or 25 mol% FA, 50 mol% chol, 25 mol% DOPC and 0.2 mol% 1,6-Diphenyl-1,3,5-hexatriene (DPH) in 300 mOsm PBS, pH 7.4, n=3 independent vesicle preparations were measured. P-values were generated by ANOVA using Dunnett's multiple comparisons test compared to no FA. **** $p \leq 0.0001$, non-significant (ns) $p > 0.5$. Error bars represent standard error of the mean.

SUPPORTING REFERENCES

1. Peruzzi, J.A., M.L. Jacobs, T.Q. Vu, K.S. Wang, and N.P. Kamat. 2019. Barcoding Biological Reactions with DNA-Functionalized Vesicles. *Angew. Chemie - Int. Ed.* 58:18683–18690.
2. Jacobs, M.L., M.A. Boyd, and N.P. Kamat. 2019. Diblock copolymers enhance folding of a mechanosensitive membrane protein during cell-free expression. *Proc. Natl. Acad. Sci.* 116:4031–4036.
3. Rawicz, W., K.C. Olbrich, T. McIntosh, D. Needham, and E. Evans. 2000. Effect of Chain Length and Unsaturation on Elasticity of Lipid Bilayers. *Biophys. J.* 79:328–339.
4. Onuki, Y., M. Morishita, Y. Chiba, S. Tokiwa, and K. Takayama. 2006. Docosahexaenoic Acid and Eicosapentaenoic Acid Induce Changes in the Physical Properties of a Lipid Bilayer Model Membrane. *Chem. Pharm. Bull. (Tokyo).* 54:68–71.
5. Simard, J.R., F. Kamp, and J.A. Hamilton. 2008. Measuring the adsorption of fatty acids to phospholipid vesicles by multiple fluorescence probes. *Biophys. J.* 94:4493–4503.
6. Dimova, R. 2014. Recent developments in the field of bending rigidity measurements on membranes. *Adv. Colloid Interface Sci.* 208:225–234.